

# CROCS: A Two-Stage Clustering Framework for Behaviour-Centric Consumer Segmentation with Smart Meter Data

Luke W. Yerbury, G. C. Livingston Jr, Ricardo J.G.B. Campello,  
Mark Goldsworthy, Lachlan O’Neil

## Abstract

With grid operators confronting rising uncertainty from renewable integration and a broader push toward electrification, Demand-Side Management (DSM) — particularly Demand Response (DR) — has attracted significant attention as a cost-effective mechanism for balancing modern electricity systems. Unprecedented volumes of consumption data from a continuing global deployment of smart meters enable consumer segmentation based on real usage behaviours, promising to inform the design of more effective DSM and DR programs. However, existing clustering-based segmentation methods insufficiently reflect the behavioural diversity of consumers, often relying on rigid temporal alignment, and faltering in the presence of anomalies, missing data, or large-scale deployments.

To address these challenges, we propose a novel two-stage clustering framework — Clustered Representations Optimising Consumer Segmentation (CROCS). In the first stage, each consumer’s daily load profiles are clustered independently to form a Representative Load Set (RLS), providing a compact summary of their typical diurnal consumption behaviours. In the second stage, consumers are clustered using the Weighted Sum of Minimum Distances (WSMD), a novel set-to-set measure that compares RLSs by accounting for both the prevalence and similarity of those behaviours. Finally, community detection on the WSMD-induced graph reveals higher-order prototypes that embody the shared diurnal behaviours defining consumer groups, enhancing the interpretability of the resulting clusters.

Extensive experiments on both synthetic and real Australian smart meter datasets demonstrate that CROCS captures intra-consumer variability, uncovers both synchronous and asynchronous behavioural similarities, and remains robust to anomalies and missing data, while scaling efficiently through natural parallelisation. These results highlight CROCS as a robust and extensible framework for advancing behaviour-centric consumer segmentation, strengthening the analytical foundations of DSM and DR strategies, and offering insights at both consumer and system levels that extend to a wide range of energy applications.

## Nomenclature

AG	Ausgrid solar home electricity dataset	GPF	Global Pattern Frequency
AMI	Adjusted Mutual Information	HAC-Wa	Hierarchical Agglomerative Clustering with Ward’s linkage
ARI	Adjusted Rand Index	JSD	Jensen-Shannon Divergence
CROCS	Clustered Representations Optimising Consumer Segmentation	KMd	<i>k</i> -medoids
DCP	Dominant Consumption Profile	PSI	Pair Sets Index
DLP	Daily Load Profile	RLP	Representative Load Profile
DR	Demand Response	RLS	Representative Load Set
DSM	Demand-Side Management	RRLS	Refined Representative Load Set
DTW	Dynamic Time Warping	SGSC	Smart-Grid Smart-City dataset
ED	Euclidean Distance	TPM	Transition Probability Matrix
EVI	External Validity Index	WSMD	Weighted Sum of Minimum Distances

## 1 Introduction

Smart metering infrastructure has proliferated globally over recent decades, with a 2021 survey finding installation programs across 47 countries targeting nearly 1.5 billion households [91]. This investment is driven by the technology’s capacity to digitise and demystify energy consumption in a transitioning energy market, enabling better informed decision-making across the energy ecosystem. In some countries, these roll-outs are approaching or have already reached maturity — for instance, the Australian Energy Market Commission requires universal smart meter deployment across the National Electricity Market by 2030 [16], meanwhile Italy is proceeding with a second-generation roll-out [92]. The resulting data deluge arrives at a critical juncture in the evolution of electrical grids worldwide.

Modern electrical systems are undergoing profound transformation, characterised by several concurrent shifts: from firm to variable energy sources, from synchronous to inverter-based resource generation, from centralised to

decentralised generation, and from passive to active consumers [17]. The increasing penetration of renewable and distributed generation introduces substantial variability and unpredictability on the supply side. Simultaneously, the electrification of transportation [118] and heating systems [98] is projected to dramatically increase demand [22, 23]. Within this changing landscape, maintaining supply-demand balance becomes increasingly complex and challenging for system operators.

There are three primary approaches for addressing supply challenges: fast-acting supply, demand-side management and energy storage [9]. Of these, Demand-Side Management (DSM) schemes, particularly Demand Response (DR) programs, are recognised as the more cost-effective solution [117]. As a result, DR has attracted significant recent attention [9, 68, 66, 79, 77, 114]. DR enables consumers to actively participate in grid management by reducing or shifting their electricity usage in response to specific signals from utilities or grid operators [68]. DR programs typically fall into two categories: price-based mechanisms like time-of-use tariffs, critical peak pricing, and real-time pricing; or incentive-based approaches such as direct load control and curtailable service [114, 77]. These programs not only promote grid reliability but also contribute to environmental sustainability by synchronising energy consumption with renewable energy availability, while providing economic benefits to participating consumers.

Effectively implementing any of the various DR programs requires a nuanced understanding of consumer behaviour. The process of collecting similar users into distinct groups, known as consumer segmentation, is key to achieving this understanding. Historically, segmentation tended to rely on contractual data, commercial classifications, and electrical parameters rather than real consumption behaviours [27, 28]. However, studies have shown that these and other demographic attributes are poor predictors of actual electricity usage, with households that appear similar on paper often exhibiting vastly different consumption patterns [114, 82]. Recent approaches overwhelmingly rely on *clustering* of smart meter time series data to form behaviourally meaningful consumer segments, where similarity is based on dynamic demand patterns rather than static traits [110, 82]. Clustering is a ubiquitous unsupervised learning technique aimed at partitioning objects from datasets into groups, such that objects within groups share a greater notion of similarity or homogeneity than objects in different groups [3, 40]. Beyond DR, consumer clustering supports a range of other applications, including load forecasting [49, 11, 58, 80], identification of energy theft [71, 78, 32], planning of energy efficiency and net metering schemes [113, 5], and anomaly detection [36].

Despite numerous methodologies being proposed for consumer clustering in the literature [68, 66, 79, 7, 46, 18, 6, 55, 8, 95, 73, 117, 90, 104, 24, 82, 111, 25, 103], current methods are constrained by one or more of the following fundamental limitations: (i) inadequate representation of the substantial intra-consumer variability observed in real-world consumption patterns, which has been recognised as an indicator of suitability for DSM and DR strategies [117, 45, 33, 53]; (ii) representing entire clusters with just one prototypical daily load profile, obscuring the shared behavioural diversity defining consumer groups; (iii) relying on temporally anchored comparisons that cannot identify consumers with similar consumption patterns when they do not exhibit such behaviours on exactly the same calendar days; (iv) sensitivity to behavioural anomalies; (v) requiring time-synchronised input data; (vi) unsatisfactory handling of missing data; (vii) sensitivity to regular discontinuities; and (viii) limited scalability to real-world populations. These shortcomings diminish the effectiveness of consumer segmentation for the aforementioned applications, consequently reducing the potential returns from the substantial investments made in smart metering infrastructure.

Addressing these limitations requires rethinking key aspects of how consumer clustering is performed. In this paper, we propose a clustering approach that, to the best of our knowledge, is unique in that it does not suffer from the above limitations. The proposed Clustered Representations Optimising Consumer Segmentation (CROCS) framework — described in more detail in Section 3, and visually summarised in Figure 1 — addresses these challenges through a novel two-stage methodology designed to more faithfully represent consumer load behaviour and enable interpretable, scalable and robust clustering for real-world datasets. The foundation of CROCS lies in recognising the 24-hour diurnal cycle as the fundamental periodic unit of electricity consumption behaviour. Accordingly, the first stage independently clusters each consumer’s Daily Load Profiles (DLP). The resulting cluster prototypes capture a compact summary of the consumer’s typical diurnal consumption patterns in a Representative Load Set (RLS). As opposed to the popular Representative Load Profile (RLP), a simple point-wise average representation for a consumer [68, 46, 117, 25, 26, 37], the RLS is a flexible unsupervised representation that can adapt to the inherent complexity of each consumer’s load behaviour, capturing intra-consumer variation in a structured and interpretable manner. Consumers with regular simple routines may require only a few representative patterns, while those with more diverse usage can be characterised by richer sets.

The second stage of the CROCS framework performs a clustering of consumers. For this, we introduce a novel set-to-set distance measure, the Weighted Sum of Minimum Distances (WSMD). The WSMD computes the dissimilarity between two RLSs, thereby capturing the dissimilarity between the two respective consumers. The WSMD computes the sum of minimum distances (using any notion of distance between short smart meter time series [115]) from elements of each set to the other, while assigning greater influence to more frequently occurring patterns. Unlike familiar set distances such as those encountered in hierarchical clustering (e.g. single or complete linkage) [3], WSMD ensures that all patterns in both sets contribute to the final similarity assessment, weighted by their rate of occurrence. The result of this second stage is a partition of consumers into groups that display similar typical

diurnal consumption patterns.

If desired, the typical behaviours common to all members of a resulting consumer cluster can then be summarised in a Refined RLS (RRLS). These are computed using a graph-based community detection approach. This method preserves the underlying similarity structure established between the relevant profiles from consumer RLSs identified during the WSMD calculations. A weighted graph is created where nodes represent consumers' prototypical load profiles, and the edges store the distances between profiles that were paired through the WSMD calculations. By detecting densely connected communities in this graph and extracting representative profiles from each community, the RRLS maintains methodological consistency while providing a concise set of patterns that characterise consumer clusters. The level of detail in the RRLS is user controlled, allowing rich or simple summaries as required for the application. The “coverage” of each profile in the RRLS is quantifiable, indicating its prevalence across both consumers and time, offering unparalleled interpretability — that is, understanding why consumers have been grouped together.

The two-stage CROCS framework addresses the previously identified challenges by: (i) capturing intra-consumer variation in the RLS, avoiding the lossy representation of behavioural diversity common to many existing clustering approaches; (ii) summarising consumer clusters with multiple diurnal profiles through the RRLS, ensuring shared behavioural diversity is captured; (iii) facilitating meaningful comparisons between similar consumers regardless of whether they present their similar consumption patterns on exactly the same days or not; (iv) reducing the impact of behavioural anomalies by weighting diurnal patterns according to the frequency with which they are exhibited; (v-vii) handling missing data, non-time-synchronised inputs, and regular discontinuities by adaptively clustering consumers' available DLPs in the first stage, without requiring temporal contiguity or alignment; and (viii) naturally supporting parallel implementation of the first-stage of clustering, supporting scalability without compromising efficacy. Beyond these practical advantages, our framework supports insights at both the consumer and system level. The availability of individualised clusterings of consumer DLPs allows for targeted analysis, such as for detecting behavioural anomalies, identifying consumers undergoing transitions (e.g., due to electric vehicle, photovoltaics or household battery uptake), or examining responses to demand-side interventions. Meanwhile, the system-level consumer segmentation supports applications such as the design and targeting of DSM schemes, DR programs, or cluster-based aggregate forecasting.

While the design of the CROCS framework was motivated by consumer segmentation in the energy domain, the same methodology could readily be extended to other forms of utility consumption, such as water [93, 61]. More broadly, it could be applied wherever long time series can be segmented into recurring periods — for example retail demand cycles, machine operation cycles, or climate cycles. The framework is also modular, allowing the use of any time series representation, distance measure, or clustering algorithm deemed effective for the domain and length of the relevant periodic subseries [115]. CROCS thus has the potential to support interpretable segmentation for a wide variety of applications beyond energy consumer segmentation.

The effectiveness of CROCS is validated through comprehensive experimental analyses using both synthetic and real-world smart meter datasets. Our experiments interrogate key components and implementation details of the CROCS framework, compare its performance against existing methodologies, and demonstrate practical utility through an application to real Australian smart meter data.

The remainder of the paper is organised as follows. Section 2 discusses related consumer clustering studies and their limitations in greater detail. Section 3 provides the mathematical formulations and implementation details of the proposed two-stage CROCS framework. Sections 4 and 5 present the experimental methodology and results respectively. Section 6 demonstrates an application of the method to a real-world dataset. Section 7 discusses implications of the experimental results. Finally, Section 8 concludes the paper.

## 2 Literature Review

This section reviews existing consumer clustering methodologies that utilise smart meter time series data. We first introduce some nomenclature for understanding the components of time series clustering approaches before discussing the methodological details of existing methods, and their associated limitations. We also discuss other multi-stage clustering frameworks for both energy consumer and general time series clustering to highlight the novelty and value of our proposed CROCS framework.

### 2.1 The Components of a Time Series Clustering Approach

Popular traditional clustering algorithms such as  $k$ -means or Hierarchical Agglomerative Clustering (HAC) were proposed to operate on objects described by orderless vectors of attributes assumed to exist in standard Euclidean space [3]. However in the age of smart meters, consumers produce time series data, where the sequential ordering of observations contains critical temporal information that should also be accounted for during the clustering process. It has been suggested that most time series clustering approaches are composed of five fundamental *components*: a data normalisation procedure, a data representation method, a distance measure, a clustering algorithm, and a prototype definition [115, 116, 4]. Studies proposing consumer clustering approaches overwhelmingly suggest alternative data

representations, as this component in particular facilitates compatibility between the complex temporal consumption data and the wealth of traditional clustering algorithms that are well-understood and readily deployable.

*Representation method* is a catch-all term for any feature extraction method or transformation of the *raw* time series which is intended to improve clustering outcomes. An effective representation should simultaneously emphasise characteristics most relevant for segmentation and reduce dimensionality, thereby moderating the influence of noise and increasing the computational efficiency of the clustering approach [4, 109]. Without appropriate representations, energy consumer clustering with long smart meter time series would be subject to the “curse of dimensionality” that renders comparisons between high-dimensional objects virtually meaningless [2].

*Distance measures* quantify the similarity between pairs of data objects, and are required for the vast majority of clustering algorithms. Typically representation methods specify a subset of compatible distances. For example, while the Euclidean Distance (ED) [3] can be applied across a swathe of different data types and representations, it is not compatible with the string-based Symbolic Aggregate Approximation [60].

A *clustering algorithm* is a procedure which utilises a data representation and distance measure to produce a partition between a set of objects, where objects placed in the same group are more similar than objects separated into different groups. The obtained partitions are typically hard or crisp, indicating that each object belongs to a single cluster, though partial cluster membership can be obtained by calling upon fuzzy or probabilistic clustering algorithms [3].

Depending on the representation, a *normalisation procedure* can be applied before and/or after the representation has been prepared from the data. Normalisation of data prior to clustering has long been deemed necessary for generating meaningful clusters [47, 83]. For time series data, normalisation is often applied independently to the individual series, as this serves to direct attention toward the shapes of the time series, rather than their amplitudes when clustering.

Finally, various *prototype definitions* have been proposed to represent or summarise the constituents of a group of objects. They are commonly utilised post-clustering for visualisations, summary purposes or as exemplars for downstream applications. They are not explicitly required for most clustering approaches, but are involved within subroutines of some clustering algorithms (e.g.  $k$ -means,  $k$ -medians and  $k$ -medoids).

It should be noted that some clustering approaches do not atomise completely into all five of these components. For instance, clustering time series with Hidden Markov Models and Expectation-Maximisation [3] does not make explicit use of any specific distance measure. Furthermore, any normalisation or prototype definition could be incorporated into this clustering approach.

## 2.2 Related Works

Table 1 presents a collection of consumer clustering approaches that have been proposed in the literature, detailing their suggested representation methods, distance measures and clustering algorithms. In the following discussion, we will focus on the representations that have been proposed, as this is where the most novelty and variation between studies appears. As can be seen in Table 1, most studies ultimately employ standard distance measures and clustering algorithms — predominantly  $k$ -means with ED.

One of the most popular representations is the RLP, which is obtained by taking the point-wise average of all DLPs in the period of interest [68, 79, 117, 25, 37]. This representation is commonly computed for DLPs produced under the same loading conditions — weekday DLPs for instance, or DLPs from the same season. Consumers represented by RLPs are then typically clustered using lock-step distance measures such as ED, and clustered with a wide variety of algorithms. Similarly, the median and 95<sup>th</sup> percentile load profiles were used in [7], instead of the average load profile.

Some studies represent consumers with features extracted from the RLPs themselves, often related to peak timing or other simple statistical descriptors [68]. Yilmaz et al. [117] and Kaur et al. [46] take the averaging process even further, suggesting to represent consumers with feature vectors composed of average consumption across 4 non-overlapping diurnal time periods, along with measures of daily variation or variation across different loading conditions. Sandels et al. [90] suggest a similar approach, though with 32 strata derived from segregating consumption according to 4 non-overlapping diurnal time periods, 4 temperature ranges and 2 day-types (weekdays and weekends). Relatedly, Meng et al. [66] use a longer vector composed of concatenated daily averages for consumption within 3 distinct diurnal time periods determined by a time-of-use tariff.

Despite some exceptions [5], it has generally been acknowledged that clustering the raw or normalised long time series is ineffective for consumer segmentation. Aside from averaging and average-based feature extraction, long time series specific features such as autocorrelations, partial autocorrelations or wavelet coefficients have also been used to represent overall temporal dependencies exhibited by consumers [7, 8, 104]. Chen et al. [24] suggested using Principal Component Analysis (PCA) components that explain at least 90% of the data variance, though this was only tested for segmenting consumers for single days of data. Another popular category of representation utilises parameters from appropriate time series models. Motlagh et al. [73] propose a Delay Coordinate Embedding (DCE) representation, which treats each consumer’s series as a dynamic system. The system’s states are represented in

Ref	Year	Representation	Clustering Approach Description <sup>a</sup>		
			Distance	Clustering Algorithm	
[68]	2024	RLP and features extracted from RLPs	ED	<i>k</i> -means, <i>k</i> -medoids, HAC (Average, Complete, Single, and Ward’s linkage) and DBSCAN	
[66]	2023	$3 \times D$ attributes representing average consumption values taken within each of 3 price segments for each of the $D$ days in the dataset	ED	<i>k</i> -means	
[79]	2023	RLP	—	Deep embedded clustering	
[46]	2022	7 attributes computed over one year of consumption	—	Gaussian mixture models	
[7]	2022	19 autocorrelation features, median or 95 <sup>th</sup> percentile diurnal profiles.	ED	<i>k</i> -means	
[5]	2022	Long time-series	Manhattan	HAC (Ward linkage)	
[8]	2020	96 autocorrelations, 96 partial autocorrelations, or 9 quantile autocovariances	ED	HAC (Complete linkage)	
[73]	2019	Delay coordinate embedding map parameters	ED	Not specified	
[117]	2019	RLPs, or mean values alongside averaged standard deviation across 4 time periods in the day	ED	<i>k</i> -means	
[90]	2019	Mean values for 32 strata (from 4 time periods in the day, 4 temperature ranges and 2 day types)	ED	<i>k</i> -means	
[104]	2018	Wavelet features or autocorrelations	ED	<i>k</i> -means	
[24]	2017	PCA features explaining at least 90% of the variance	ED	<i>k</i> -means	
[111]	2016	Markov state transition probability matrices computed on a Symbolic Aggregate Approximation of the load data ( $3 \times 3$ for each of 4 time periods in the day)	Kullback-Leibler Divergence	Clustering by Fast Search and Find of Density Peaks	
[25]	2012	RLP	Minkowski Metric with $p = 1, 2, 3, 4, 5$	<i>k</i> -means, Fuzzy <i>c</i> -means, Follow the Leader, HAC (Average and Single linkage)	

<sup>a</sup>Density-Based Spatial Clustering of Applications with Noise (DBSCAN), Euclidean Distance (ED), Hierarchical Agglomerative Clustering (HAC), Principal Component Analysis (PCA), Representative Load Profile (RLP)

Table 1: Studies that have proposed consumer clustering approaches, and the representation methods, distance measures and clustering algorithms of which they are composed. These methods all utilise a single stage of clustering, while other multi-stage methods are collected in Table 2.

the phase space and modelled via a mapping strategy, whose parameters are then used to represent consumers and assess their similarity. Wang et al. [111] propose modelling consumption across four regular diurnal periods using Markov sequences. They employ the Symbolic Aggregate Approximation to discretise consumption into states, then fit transition probability matrices for each of the four periods, using Kullback-Leibler divergence to assess consumer similarities.

Our CROCS framework is not the first to employ multiple stages of clustering for consumer segmentation — or indeed, for time series clustering more generally. Sun et al. [95] and Tsekouras et al. [103] both proposed two-stage frameworks for clustering energy consumers. Sun et al. [95] suggested an ensemble clustering approach, where the first stage produced many partitions of consumers by clustering their DLPs independently on each day of the relevant period using *k*-means with ED. These daily partitions were then amalgamated into a similarity matrix indicating how frequently households were grouped together, with a final spectral clustering performed on this matrix to produce the definitive consumer segmentation. On the other hand, the first stage of the method proposed by Tsekouras et al. [103] clusters the DLPs of each consumer independently, as for our CROCS framework. They select the optimal partition for each consumer obtained from *k*-means, adaptive vector quantisation, fuzzy *c*-means and HAC by optimising a set of six Relative Validity Indices (RVIs) (such as the Davies-Bouldin Index). However, unlike CROCS, for the second stage of clustering they suggested that a single prototypical load profile be selected to represent each consumer. This profile was primarily taken as the prototype of the cluster with highest membership — for this reason we refer to this form of consumer representation as the Dominant Consumption Profile (DCP). However, the authors do suggest that the cluster with some other characteristic, such as peak load demand, could be used instead.

Table 2 collects two-stage methods that have been proposed in the literature, categorising them according to their end-goal — either consumer segmentation or load profile clustering. This includes methods that have been proposed in the broader time series clustering literature, with their end-goals interpreted in terms of smart meter clustering. Unlike consumer segmentation, load profile clustering is concerned with the segmentation of DLPs, regardless of which consumers produced them on which days. Many more two-stage methods have been proposed for load profile clustering than for consumer segmentation. Two-stage methods for load profile clustering are typically implemented in one of two ways. Refinement methods operate as for the first stage of CROCS, independently clustering the DLPs of each consumer individually. However, the second stage then proceeds to cluster all prototypes from all consumers, seeking to find common diurnal patterns exhibited across the board. Hierarchical methods on the other hand will cluster DLPs within the groups obtained from the first stage of clustering, often using a different method to capture different characteristics at each level.

For consumer clustering, we have categorised the daily ensemble method of Sun et al. [95] as an ensemble-based

Categorisation	Stage One	Stage Two	Energy Domain References	General Time Series References
Consumer Clustering				
Representation	Within-consumers	Consumers	[103], CROCS	—
	Pooled	Consumers	—	[75], [57]
Ensemble	Consumers	Consumers	[95]	—
Load Profile Clustering				
Hierarchical	Within-consumers	Pooled	[107], [18], [1], [67], [56], [53]	—
	Pooled	Pooled	[100], [99]	[108], [119]
	Consumers	Pooled	—	[54]

Table 2: Studies that have proposed two-stage clustering methodologies for general time series and smart meter data specifically. Note that we have categorised the general time series methods as they would be applied to the clustering of smart meter data. Note that for the different stages: “Within-consumers” refers to clustering the DLPs (or recurrent sub-periods) of each consumer (or long time-series) independently; “Consumers” refers to clustering the consumers (or long time-series); and, “Pooled” refers to clustering the DLPs (or recurrent sub-periods) altogether, without regard for which consumer produced the DLP and when.

two-stage method, and the DCP-based method of Tsekouras et al. [103] as representation-based. The purpose of the first stage of clustering in a representation-based two-stage method is to learn an appropriate representation to use for subsequently clustering the consumers (i.e. the whole time series) in the second stage of clustering. Our proposed CROCS framework and the DCP approach suggest that this representation should be local, that is, learned independently for each consumer. However, Nakashima et al. [75] and Li et al. [57] propose two-stage clustering methods for general application which instead utilise a global representation. Speaking in the context of smart meter time series, these methods first perform a load profile clustering, finding common consumption patterns exhibited in DLPs across all consumers on all days. By clustering all DLPs in this “pooled” manner, consumers can then be represented according to the frequency with which they display the discovered prototypical patterns. In particular, both of these studies utilise proportion or count vectors to represent consumers, which indicate how frequently each consumer’s DLPs were found to belong to each of the global clusters. We refer to this form of consumer representation as the Global Pattern Frequency (GPF) representation.

### 2.3 Limitations of Existing Studies

Having conducted a review of the literature, we have identified several limitations that variously affect existing single- and multi-stage consumer clustering approaches. We now discuss each of these limitations in turn.

#### (i) Inability to reflect intra-consumer variation

The success of consumer clustering depends critically on how each consumer’s long load time series is represented for comparison [73]. While computationally efficient and easy to interpret, it has been widely acknowledged that aggregation-averaging processes, such as is used to create RLPs, miss the substantial intra-consumer variability observed for real-world consumers [115, 81, 73, 117, 82, 45, 56, 64]. Individual consumers can exhibit diverse usage behaviours from day to day, such that if clustered, their DLPs would belong to different clusters on different days [115, 117, 56]. Furthermore, averaging across these distinct behaviours can result in RLPs that are not only unrepresentative of any constituent DLPs, but may also lie in low-density regions of the data space — particularly if the DLP distribution is non-convex [56].

Alternative representations that process the entire long time-series — such as those using autocorrelations, Markov model parameters or delay coordinate embedding map parameters — may capture specific aspects of overall temporal variation (like periodicity, state transitions, or attractor dynamics) and avoid direct averaging, but they still fundamentally compress multi-modal behavioural landscapes into fixed-length feature vectors. This compression obscures the explicit structure of distinct behavioural modes, making their shapes, prevalence, and relationships not directly accessible from the representation.

The aforementioned two-stage consumer clustering approaches are better equipped to avoid this limitation. For instance, the daily ensemble clustering method from Sun et al. [95] and the GPF approaches from Nakashima et al. [75] and Li et al. [57] allow consumers to belong to different clusters on different days. Meanwhile, the DCP method from Tsekouras et al. [103] still only uses a single profile for consumer segmentation in the second stage. In doing so, the method fails to take full advantage of the rich representation discovered in the first stage of independent consumer DLP clustering.

Because intra-consumer variability has been recognised as an indicator of suitability for DSM strategies [117, 45, 33, 53], clustering methods that fail to account for intra-consumer variability may miss important distinctions among consumers that are particularly relevant for DR programs. An effective clustering approach for consumer segmentation must therefore capture key within-consumer behavioural diversity and allow the clustering process to take this facet into account.

#### (ii) Inability to represent common intra-consumer variation in clusters

In parallel with the tendency for existing methods to summarise individual consumer behaviour over long periods using a single RLP, by default most clustering approaches summarise the behaviour of entire groups of consumers in a single prototypical DLP [68, 66, 79]. The dominant approach is to reduce the load data across  $m$  consumers and  $p$  days into  $k$  clusters (with  $k \ll m$ ), each represented by one characteristic DLP [73]. If the intra-consumer variability missed by a singular RLP is substantial, then the behavioural diversity missed when summarising multiple consumers with a single profile is likely even more pronounced. This reduction is not necessarily an explicit design choice optimised for applications of consumer segmentation; rather, it is likely driven by the default structure of conventional clustering pipelines, which lack the capacity to summarise a cluster by more than one prototype.

While it is certainly impractical and unproductive to capture every nuance of a group's behaviour, there is value in allowing more than one representative profile per cluster — particularly in cases where a group of consumers exhibit the same set of distinct behavioural modes. A more expressive approach to group representation can reveal important behavioural differences relevant to DR program design. For example, one group of consumers may exhibit a dominant usage pattern on 90% of days, while consumers from another group alternate between two primary behaviours with nearly equal frequency (e.g., 45% and 40%). Although both groups exhibit internal consistency, the second group's multi-modal behaviour is poorly captured by a single prototype. While existing methods may suffice for the first group, program designers may achieve greater success by accounting for the shared behavioural diversity expressed in the second group.

#### (iii) Inability to identify similar consumers on asynchronous schedules

Another shortcoming of many consumer clustering approaches lies in their reliance on *temporally anchored comparisons* — that is, consumer usage tends to be compared on strictly the same calendar days, often as a result of aligning long consumption series in time. This framing assumes that behavioural similarity must be expressed concurrently in order to be meaningful for segmentation applications. However, for many DSM and DR applications, it is not critical whether two consumers exhibit similar usage patterns on exactly the same day, but rather whether they exhibit similar patterns at all.

In practice, similar diurnal consumption behaviours may manifest on different days depending on consumers' schedules and routines. This is particularly relevant in the residential sector, which accounts for roughly a quarter of final electricity consumption in both Australia and the EU [14, 35], and represents a major untapped source of DSM and DR flexibility [77]. Unlike the regularity of commercial and industrial demand, residential usage is increasingly shaped by varied employment arrangements. In Australia, for instance, only about 60% of workers follow a standard Monday–Friday schedule, with the remainder engaged in non-standard, casual, flexible, or shift work; additionally, over a third of employees now usually work from home, a proportion that has risen since the Covid-19 pandemic and is projected to continue growing [15, 50, 76]. In practice, this means consumers may be behaviourally equivalent yet out of sync in time — a similarity that temporally anchored approaches are poorly equipped to capture.

Temporally anchored clustering approaches include long time series methods which rely on order-sensitive features such as frequency-domain features, or time series model coefficients. These long series approaches are typically implemented using synchronised input windows, and are sensitive to the order in which behaviours are expressed across diurnal cycles. Even representing consumers by their raw long time-series and using elastic distance measures such as Dynamic Time Warping (DTW) [42], which introduce a degree of local warping, maintains temporal anchoring of consumer series globally. Meanwhile, the ensemble method from Sun et al. [95] is the only two-stage method that enforces temporal anchoring. While not temporally anchored, the DCP representation could only identify asynchronous similarity between consumers if by chance they share the same dominant pattern, with multi-modal similarity likely to be missed.

By enforcing calendar alignment, these methods can fragment otherwise coherent groups of consumers, particularly in residential settings where routines are increasingly asynchronous. This limits the effectiveness of segmentation and undermines the value of DSM and DR initiatives for both retailers and consumers.

#### (iv) Sensitivity to behavioural anomalies

Most existing consumer clustering approaches implicitly assume that all the constituent DLPs within a consumer's time series are equally informative for grouping, assigning them identical weight during feature extraction or similarity calculations. However, real-world electricity consumption includes anomalous days [115, 73], which may arise due

to special occasions, travel, illness, temporary changes in household occupancy, equipment malfunction or other irregular events. While some of these events constitute a legitimate part of a consumer's usage history, they are typically non-representative of routine behaviour and are usually less relevant for downstream applications. When clustering methods fail to differentiate between typical and atypical usage, even just a few of these behavioural anomalies can exert disproportionate influence over the representation of a consumer, allowing the clustering process to be biased undesirably [73].

This issue is particularly pronounced for crude dimensionality reduction techniques, such as RLPs or feature extraction methods like Principal Component Analysis [73], where anomalous behaviours become embedded in the consumer's representation and cannot be disentangled from typical patterns. While one could attempt to mitigate this sensitivity by removing days with extreme values or irregular patterns prior to clustering, a more robust approach would assign greater weight to the most prevalent and stable patterns of behaviour within each consumer's DLP distribution, while appropriately downweighting atypical behaviour. By shifting the focus onto recurring patterns, and reducing the influence of outliers, clustering can produce more interpretable and actionable groupings, while still acknowledging the full spectrum of behavioural diversity.

#### **(v) Requiring time-synchronised input data**

Many consumer clustering approaches require time-synchronised input windows, meaning all series must start and end at the same timestamp with no temporal offsets [73]. This constraint becomes problematic when consumers have different quantities of available historical data. Such a scenario is commonly encountered in incomplete deployment programs, where installation dates will vary between consumers. Yet, this scenario will persist indefinitely as households relocate, resetting the quantity of relevant historical data.

Techniques relying on globally computed representations, such as matrix factorisation (PCA or Singular Value Decomposition) expressly require equivalent input windows to operate. Many local representations such as the Discrete Fourier Transform, Discrete Wavelet Transform, or Symbolic Aggregate Approximation still require uniform-length inputs to generate compatible representations, as input length directly determines the dimensionality of the resulting representations. Similarly, using the long time-series directly necessitates equal-length inputs. For these methods, this limitation forces either truncation of valuable historical data or exclusion of newer consumers with limited history, ultimately reducing the representativeness and inclusivity of the resulting segmentation. Two-stage methods (excepting Sun et al.'s daily ensemble approach [95]) and model-based methods such as Motlagh et al.'s [73] DCE where models have a fixed number of parameters can more naturally circumvent this limitation.

#### **(vi) Sensitivity to regular discontinuities**

For DR programs such as time-of-use tariffs, many energy retailers will make a distinction between weekdays and weekends for residential consumers due to the significance of commercial consumption during weekdays [48]. Some methods are not well-suited to clustering long time series with the sorts of discontinuities that arise when clustering weekday and weekend consumption patterns separately, i.e. if concatenating all weekday usage in a single time series. These gaps can introduce spurious temporal dependencies and distort the underlying structure of the data, potentially misleading the clustering process. For example, frequency-based representations such as Discrete Fourier Transform or Discrete Wavelet Transform, time series models, or autocovariance-based representations may become unreliable when applied to discontinuous time series. However, RLPs and two-stage methods are naturally more equipped to handle this scenario.

#### **(vii) Unsatisfactory handling of missing data**

Periods of missing data can arise due to device malfunctions, communication interruptions, or other unknown reasons [41, 52, 88]. While shorter periods are reasonable candidates for imputation, it is also common to simply remove significantly affected records [31]. In the context of consumer clustering, the extent of record removal that is required depends on the consumer representation method. The aforementioned methods that require time-synchronised or continuous input cannot abide by the minimal removal of individual affected days, requiring instead that the consumer be dropped from the analysis altogether. On the other hand, RLPs, and two-stage methods that first cluster consumer DLPs or pooled DLPs are more robust to the removal of affected days, and maintain greater generalisability and representativeness by including the maximum amount of reliable data.

#### **(viii) Limited scalability to real-world populations**

As smart meter deployments continue to expand globally, data mining methods capable of efficiently operating at realistic scales are becoming increasingly important. However, a balance must be struck, as scalability should not come at the cost of significant compromises to efficacy. Many of the proposed consumer clustering approaches seemingly prioritise computational efficiency by applying coarse dimensionality reduction techniques — like the

aforementioned use of averaging to obtain RLPs or short feature vectors. As previously discussed, this sacrifices behavioural nuance and reduces clustering efficacy, ultimately diluting the potential impact of DSM and DR programs.

The scalability of consumer clustering approaches largely depends on whether they employ globally or locally fitted representations. Methods employing global representations, such as GPF or PCA face greater computational challenges than those using local representations fitted independently to each consumer. This is because global methods must jointly process data across all consumers, resulting in memory and computational demands that scale poorly with the number of consumers or the length of their time series. Moreover, when new consumers are added to a dataset, global representations need to be recomputed in full, further undermining their practicality in continuously expanding deployments. In contrast, local methods decouple the representation step across consumers and naturally support parallel implementations. They also adapt more readily to expanding datasets, since representations can be updated independently for each new consumer without requiring recomputation across all consumers.

Consider for instance two-stage methods utilising global representations. The GPF representation proposed by Li et al. [57] requires clustering all DLPs from all consumers simultaneously, while Nakashima et al.'s [75] GPF approach requires clustering all subsequences generated by a fixed-size sliding window applied to all consumer time series. In contrast, RLPs, DCPs autocovariances, wavelet coefficients, time series models, and CROCS support per-consumer processing for their local representations. This makes them more robust to scaling in terms of both the number of consumers and the volume of data per consumer, and more serviceable in streaming scenarios than their global counterparts.

Despite the growing need for scalable solutions that maintain representation quality, relatively few studies engage meaningfully with this trade-off [68, 20]. A robust consumer clustering methodology must therefore achieve computational efficiency without sacrificing segmentation accuracy, ultimately capitalising on the substantial investment made in smart metering infrastructure and maximising impact in downstream applications.

### 3 CROCS: The Two-Stage Consumer Clustering Framework

Designed to avoid the aforementioned limitations of existing methodologies, we propose a novel two-stage clustering framework: **Clustered Representations Optimising Consumer Segmentation (CROCS)**. Figure 1 visually summarises both stages of the proposed framework, with further discussion and details provided throughout the remainder of this section.

#### 3.1 Stage One: Clustering Consumers' Daily Load Profiles

Broadly speaking, the first stage of our proposed methodology clusters periodic units of individual long time series that are relevant for the analysis at hand. Depending on the domain, these periods could span seconds, minutes, hours, days, weeks, months, quarters or years. For example, machine operation cycles could produce periodic time series with short periods measured in minutes, retail demand may produce time series with weekly periods, and agricultural yields with yearly periods. While smart meter time series may contain various periods (e.g. weeks or years) that could be clustered in the first stage of the CROCS framework, we cluster the 24-hour diurnal period as it is the fundamental periodic unit of energy consumption.

We now consider a dataset containing long time series produced by  $m$  distinct entities. Suppose that we have observed  $p_i$  periods for the  $i^{\text{th}}$  entity, with  $\phi$  measurements per period, taken at regular intervals. Acknowledging that our methodology could be applied to other time series fitting this format, we shall proceed with our discussion in the context of smart meter time series where  $m$  represents the number of distinct consumers,  $p_i$  represents the number of days of data considered for the  $i^{\text{th}}$  consumer, and  $\phi$  relates to the sampling frequency of the observations (e.g.  $\phi = 24$  or  $48$  for hourly or half-hourly sampling rates respectively). The  $i^{\text{th}}$  consumer's long time series can then be represented as  $\mathbf{x}_i = [x_{i,1} \ x_{i,2} \ \dots \ x_{i,\phi} \ x_{i,\phi+1} \ x_{i,\phi+2} \ \dots \ x_{i,2\phi} \ x_{i,2\phi+1} \ x_{i,2\phi+2} \ \dots \ x_{i,p_i\phi}]$ , where  $x_{i,j}$  is the energy consumption of the  $i^{\text{th}}$  consumer through time  $j$ . Equally, with the  $i^{\text{th}}$  consumer's  $\ell^{\text{th}}$  DLP represented as  $\mathbf{x}_i^\ell = [x_{i,\ell\phi+1} \ x_{i,\ell\phi+2} \ \dots \ x_{i,\ell\phi+\phi}]$  for  $\ell \in \{0, 1, \dots, p_i - 1\}$ , we can instead consider the set of each consumer's DLPs, as given by  $\mathcal{S}_i = \{\mathbf{x}_i^0, \mathbf{x}_i^1, \dots, \mathbf{x}_i^{p_i-1}\}$ .

In the first stage of CROCS, clustering is applied independently to each consumer to obtain a partition of  $\mathcal{S}_i$  for each  $i \in \{1, 2, \dots, m\}$  into  $k_i$  clusters<sup>1</sup>. This independence makes this stage straightforward to parallelise across consumers, offering greater computational efficiency when scaling to larger populations. As depicted in Figure 1, the number of clusters composing the RLS can vary from consumer to consumer, or it can be fixed for all consumers. If allowed to vary, the number of clusters can be selected autonomously using an appropriate RVI [116]. This is the methodology applied in the similar first stage of the DCP-based approach in Tsekouras et al. [103]. A simpler and more robust approach to the selection of  $k_i$  that fixes the same value ( $k$ ) for all consumers is discussed in Section 5.1.

<sup>1</sup>Note that these are assumed to be *hard* partitions. Consider a set  $\mathcal{X} = \{\mathbf{x}_1, \mathbf{x}_2, \dots, \mathbf{x}_m\}$ . A hard partition of  $\mathcal{X}$  is a collection of  $k$  subsets  $\mathcal{C} = \{\mathcal{C}_1, \mathcal{C}_2, \dots, \mathcal{C}_k\}$  such that  $\bigcup_{i=1}^k \mathcal{C}_i = \mathcal{X}$ , all  $\mathcal{C}_i \neq \emptyset$ , and  $\mathcal{C}_i \cap \mathcal{C}_j = \emptyset$  for  $i \neq j$ , where  $\emptyset$  is the empty set.

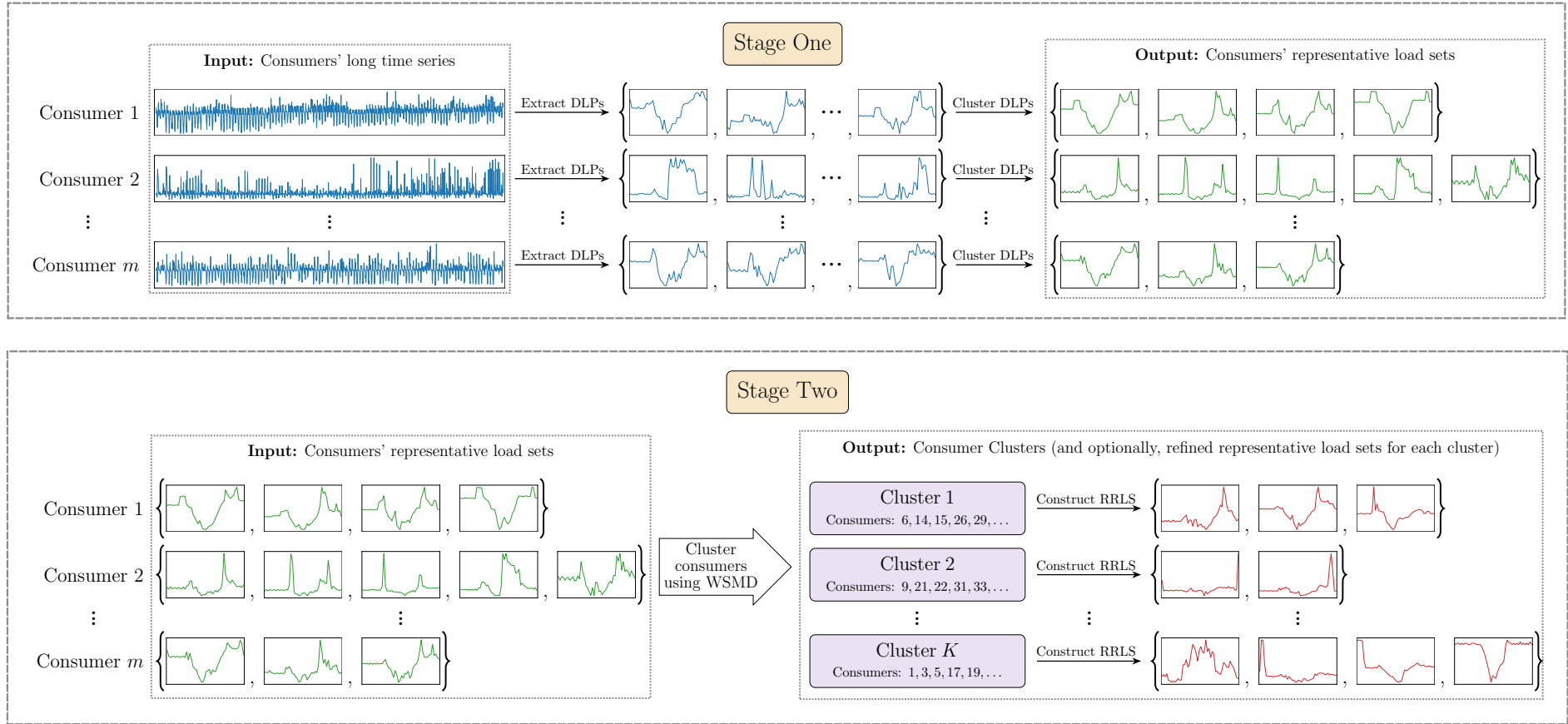


Figure 1: A visual depiction of the two-stage CROCS framework.

Subsequently, the resulting prototypes for each consumer are contained in their RLS,  $\hat{\mathcal{S}}_i = \{\pi_i^1, \pi_i^2, \dots, \pi_i^{k_i}\}$ . Note that each prototype  $\pi_i^j$  in the RLS represents a cluster containing  $n_i^j$  DLPs, such that  $\sum_{j=1}^{k_i} n_i^j = p_i$ .

CROCS should be regarded primarily as a framework for approaching consumer clustering. As such, we do not prescribe any particular clustering approach (i.e. normalisation procedure, representation method, distance measure, clustering algorithm and prototype definition) be used within it — the framework is compatible with any of the plethora of existing clustering components. For a comparison of representation methods, distance measures and clustering algorithms applied specifically for clustering DLPs as in stage one of our framework, we direct the reader to our previous comparative study [115]. Meanwhile, the aforementioned prototypes could be for instance average, medoid or median profiles as the practitioner deems optimal for the given application. Furthermore, aligning with an earlier point regarding the utility of normalisation to direct a clustering algorithm to find similarity based on shape rather than magnitude, we recommend some form of normalisation (e.g. min-max or  $z$ -normalisation [116]) be applied to the DLPs prior to clustering.

### 3.2 Stage Two: Clustering Consumers

The second stage of the CROCS framework clusters the long time series, or by proxy, the entities they represent. In our context, those entities are energy consumers represented by the long time series  $\mathbf{x}_i$ . Unlike the first stage, this second stage makes use of one particular representation method — that is, the RLSs ( $\hat{\mathcal{S}}_i$ ) obtained from the first stage of clustering.

Comparing consumers via their RLSs requires a distance measure tailored to their structure, and for this purpose we introduce WSMD. WSMD extends the original Sum of Minimum Distances [34] by incorporating information about the size of the clusters represented by each prototype in  $\hat{\mathcal{S}}_i$ . In doing so, it ensures that all prototypes contribute to the pairwise consumer dissimilarities in proportion to the frequency of the behaviours they capture.

In particular, suppose that  $d(\cdot, \cdot)$  is a time series dissimilarity measure that can be applied to DLPs, then the WSMD between  $\hat{\mathcal{S}}_i$  and  $\hat{\mathcal{S}}_j$  is given by

$$\Delta_{\text{WSMD}}(\hat{\mathcal{S}}_i, \hat{\mathcal{S}}_j) = \frac{1}{2} \left[ \frac{1}{p_i} \sum_{a=1}^{k_i} n_i^a \min_b d(\pi_i^a, \pi_j^b) + \frac{1}{p_j} \sum_{b=1}^{k_j} n_j^b \min_a d(\pi_j^b, \pi_i^a) \right].$$

For each prototype in a consumer's RLS, WSMD finds the closest prototype from the other consumer's RLS. The distance between consumers is then taken as the weighted average of these minimum distances. While any time series dissimilarity measure can be used within the WSMD, consistency can be achieved by using the same measure as was used to cluster consumer DLPs in the first stage. A WSMD computation between two consumers has been visualised in Figure 2, where

$$\begin{aligned} \Delta_{\text{WSMD}}(\hat{\mathcal{S}}_i, \hat{\mathcal{S}}_j) = \frac{1}{2} \left[ \frac{1}{180} (28 \cdot 0.739 + 72 \cdot 0.850 + 46 \cdot 0.733 + 34 \cdot 1.161) \right. \\ \left. + \frac{1}{180} (32 \cdot 0.739 + 85 \cdot 0.850 + 63 \cdot 0.733) \right] = 0.825. \end{aligned}$$

The second stage of the CROCS framework then achieves a partition of consumers into clusters by pairing the WSMD distance measure and RLS representation method with any existing clustering algorithm.

### 3.3 Computing Refined Representative Load Sets

Consumer clustering methods often struggle to provide interpretable and meaningful explanations for why particular consumers have been grouped together, often leaving practitioners with little insight into what shared behavioural patterns define consumer groups. The CROCS framework addresses this interpretability challenge by offering practitioners the option of generating a Refined Representative Load Set for each consumer cluster. Each RRLS contains one or more prototypical DLPs that describe the various ways that consumers within a cluster typically use their energy. Unlike single-prototype cluster summaries, the RRLS summary more accurately captures distinct behavioural modes shared among consumers within a cluster. Furthermore, the frequency, or “coverage” of each hyperprototype is quantifiable, indicating its prevalence across both consumers and days. This optional summary step in the CROCS framework transforms opaque consumer cluster assignments into interpretable behavioural profiles, enabling practitioners to understand not just which consumers belong together, but precisely what diurnal consumption patterns they share.

The process of computing an RRLS for an individual cluster of consumers is depicted in Figure 3. To begin, the prototype graph or network induced by all included consumers' pairwise WSMD computations is constructed. In

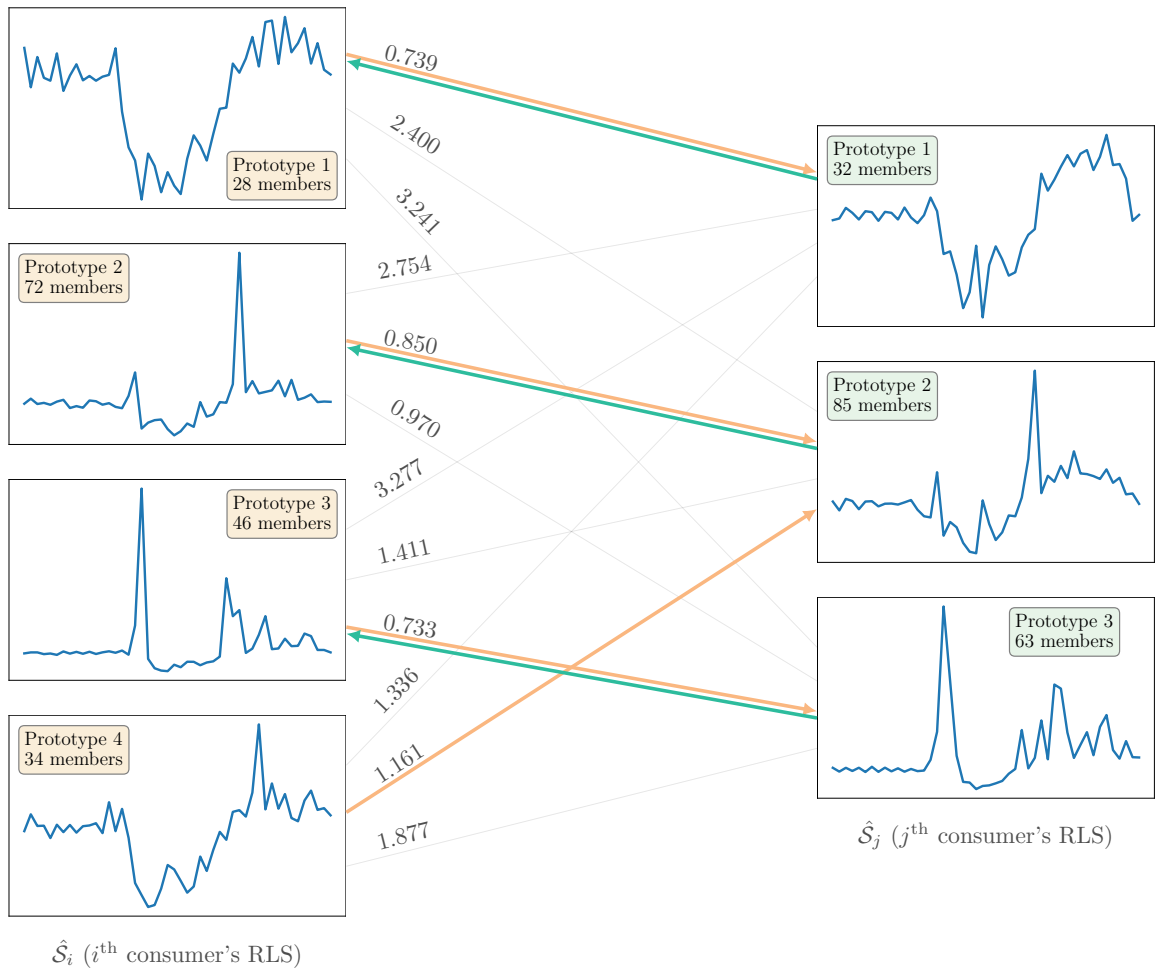


Figure 2: A visualisation of the WSMD set distance measure being applied to a pair of consumer representative load sets.

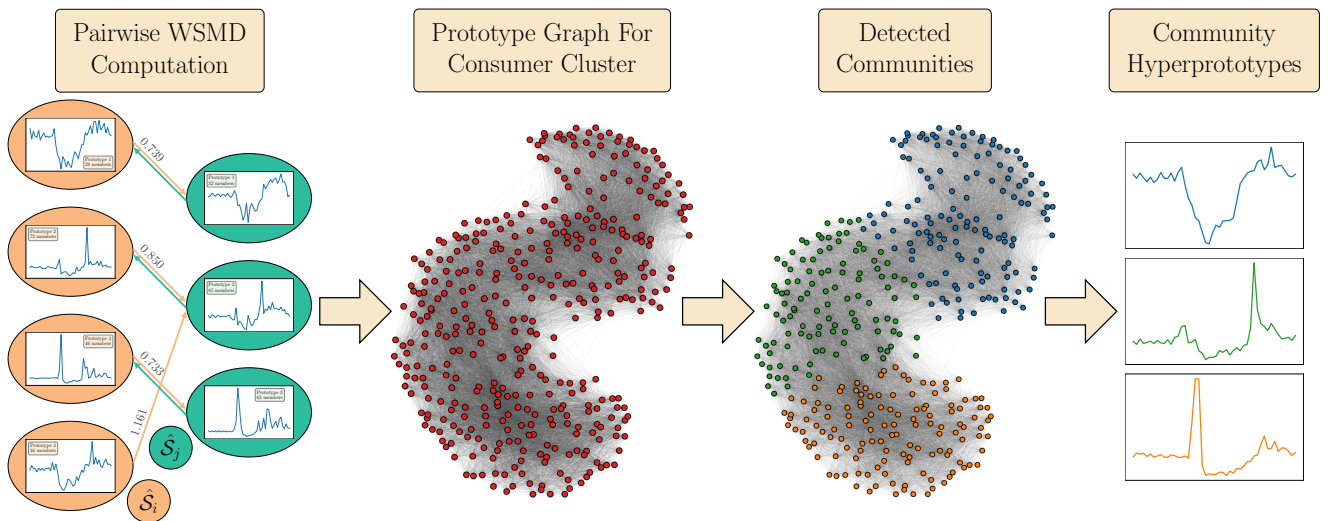


Figure 3: A visualisation demonstrating computation of the RRLS hyperprototypes for consumer clusters.

such a graph, the vertices represent the consumers' RLS prototypes, and the edges reflect the *directional* connections discovered between those prototypes by WSMD, i.e. the coloured edges shown in Figure 2. These directed edges are weighted according to the pairwise dissimilarity of the prototypes. However, because WSMD utilises a dissimilarity measure  $d(\cdot, \cdot)$ , and smaller dissimilarities should correspond to stronger connections, an appropriate transformation must be applied to convert the dissimilarities into similarities — for example, by assigning weights as  $1/d(\cdot, \cdot)$ <sup>2</sup>. Furthermore, the vertices are weighted according to the number of DLPs represented by each consumer prototype. For instance in Figure 2, the vertex representing prototype 4 for the  $i^{\text{th}}$  consumer (bottom left) would have a weight of 34. Additionally, a directed edge would exist to consumer  $j$ 's 2<sup>nd</sup> prototype (middle right) with a weight of  $1/1.161 = 0.861$ .

Densely, or strongly, connected regions of these prototype graphs represent shared modes of usage within the consumer cluster. Identifying these densely connected sub-graphs allows us to compute refined prototypical diurnal profiles that capture those shared modes of usage. Thus with the prototype graph constructed, any community detection algorithm compatible with weighted directed graphs can be applied to obtain a partition of the vertices [38, 39], as depicted in the third panel of Figure 3. For each detected community, a corresponding hyperprototype is obtained (depicted in the fourth panel of Figure 3) as the prototype of the included vertices.

The number of distinct consumers and days covered by the vertices in each community provides an indication of the coverage of the corresponding hyperprototypes. While practitioners can choose the number of communities (i.e. the number of hyperprototypes in the RRLS) to suit their application — allowing for either concise or detailed behavioural summaries — the quantification of coverage is most meaningful when seeking to identify the natural number of behavioural modes present in the data. However, using medoid prototypes offers an effective approach for representing core consumption patterns while remaining robust to occasional anomalous behaviours, thereby reducing sensitivity to the choice of number of communities.

Whilst an argument could be made for simply applying a time series clustering approach to the union of all constituent consumer RLSs instead, this graph-based approach preserves the explicit relationships established during the WSMD computation, maintaining methodological consistency between the consumer clustering and hyperprototype extraction. For intuition, consider the ideal scenario where consumers in a cluster share exactly  $n_c$  similar consumption patterns. Stage one clustering would ideally discover these patterns, resulting in each consumer being represented by  $n_c$  prototypes in their RLS. Hence the resulting prototype graph would be composed of exactly  $n_c$  connected components. With each of the connected components readily identifiable as a community, the consumer cluster would then be described by an RRLS with  $n_c$  hyperprototypes — one per common consumption behaviour. In reality, the prototype networks will be much more complex, but the underlying principle remains: densely connected regions of the prototype graph reveal the core behavioural modes that unite consumers within a cluster.

## 4 Experimental Setup

This section presents the datasets, metrics, and implementation details used to evaluate CROCS in our subsequent experiments.

### 4.1 Real Data

Throughout the course of our experiments we make use of two publicly available Australian smart meter datasets: the Ausgrid Solar Home Electricity (AG) dataset [12, 84] and the Smart-Grid Smart-City (SGSC) dataset [13].

The AG dataset comprises 300 households in New South Wales with rooftop photovoltaic (PV) systems, each with 1,096 half-hourly sampled DLPs recorded between 1st July 2010 and 30th June 2013. Meters separately recorded gross household consumption, PV generation, and (for some households) an off-peak controlled load. In line with typical interval metering — which records combined imports and exports rather than separately metered consumption and generation — we derived net household demand by combining general and controlled load and subtracting PV generation.

The SGSC dataset was used in the form prepared by [87], where extensive pre-processing and filtering was applied. The resulting subset comprises 3,953 households in New South Wales, each with 365 half-hourly DLPs from 1 January to 31 December 2013, also representing net household demand.

### 4.2 Synthetic Data

We also present results from experiments using synthetic datasets, where a ground truth partition is available. For this purpose we employed the synthetic DLP generator introduced in [115]. This generator produces min-max normalised half-hourly DLP instances that conform to one of 20 fundamental cluster *shapes*. Using the baseline

<sup>2</sup>While such transformations are required for a majority of community detection algorithms, some methods have been proposed that directly operate on dissimilarities (or length data) as edge weights [72], i.e. smaller edge weights are interpreted as stronger connections.

parameter settings specified in [115], the generator produces unique profiles through a stochastic process, while ensuring profiles derived from the same shape form recoverable clusters. The 20 shapes represent distinct residential consumption patterns, differing by the timing, number, shape and relative magnitude of peak consumption events. The generator is also capable of producing outlier DLPs that don't conform to any of the 20 cluster shapes with high probability, and don't form clusters of their own.

To construct a synthetic dataset, the specified number of consumers were distributed among  $K^*$  true clusters, with cluster sizes drawn from a multinomial distribution with uniform probabilities, emulating a balanced consumer distribution across clusters. Each synthetic consumer cluster was defined by drawing a unique subset of  $k^*$  DLP shapes from the available 20, ensuring that no two consumer clusters had identical sets of defining shapes. For each consumer, DLPs were then generated as new instances from random shapes within their cluster's subset until the required number of days was obtained. As required, a controlled number of those profiles ( $n_O$ ) were instead designated to be outliers that didn't conform to any of the 20 shapes. Further details regarding the composition of the synthetic datasets will be provided as the experiments are introduced.

The accuracy with which synthetic consumer clusters were recovered was measured using three External Validity Indices (EVIs): Adjusted Rand Index (ARI) [43], Adjusted Mutual Information (AMI) [105], and Pair Sets Index (PSI) [86]. These indices represent three complementary methodological categories for comparing partitions — pair-counting (ARI), information-theoretic (AMI), and set-matching (PSI) respectively [106]. ARI and AMI are widely recommended due to their adjustment for chance and independence from the number of clusters [69, 94, 44], while PSI is also chance-corrected and uniquely sensitive to errors in both small and large clusters. Given their different formulations, agreement among ARI, AMI, and PSI demonstrates that our conclusions are robust to the choice of evaluation index. For conciseness, we only reported ARI values where all three measures yielded consistent results.

### 4.3 CROCS Configuration

As previously discussed, CROCS could be configured to use any of the plethora of clustering approaches and components from among the clustering literature. We will now discuss the specific configuration that we elected to use throughout our experiments.

The first stage of CROCS was implemented with min-max normalisation, applied independently to each DLP. This is a very common normalisation procedure in the smart meter time series clustering literature [68, 104, 24, 111, 103], and ensures that DLPs range within the interval  $[0, 1]$ . Dynamic Time Warping (DTW) [89] with a 1 hour warping window (denoted as DTW-2 for half-hourly data) demonstrated strong performance for clustering of half-hourly DLPs specifically in our previous comparative study [115] when combined with either Hierarchical Clustering with Ward's linkage (HAC-Wa) or  $k$ -medoids (KMd) [3]. Accordingly, DTW-2 is utilised with these algorithms by default. Finally, medoid prototypes have been used to populate RLSs to avoid the aforementioned issue with pointwise means whereby the mean can lie in low-density regions of the data subspace and fail to be adequately representative of the discovered cluster.

Whilst not strictly necessary, we have elected to use the same clustering algorithm in the second stage of CROCS as was used in the first stage. We used the Python package `aeon` for DTW, `sklearn_extra` for KMd (using the partitioning around medoids method), `sklearn` for  $k$ -means, and both `scipy` and `fastcluster` for HAC-Wa. Both KMd and  $k$ -means were run with 30 initialisations and a maximum of 200 iterations, using the  $k$ -medoids++ and  $k$ -means++ initialisation schemes respectively [10]. Additional details specific to particular experiments are provided in context.

## 5 Results

### 5.1 Stage One: How many clusters?

A fundamental consideration when implementing the CROCS framework concerns the selection of  $k_i$ , or the number of clusters to extract from each consumer's set of DLPs in stage one. This parameter directly controls the size and representational complexity of each consumer's RLS. While it is certainly possible to individually optimise  $k_i$  for each consumer using RVIs as in [103], investigation reveals a surprisingly robust alternative:

Overestimate  $k_i$ , using the same value for all consumers — simply  $k$ .

This approach increases the likelihood that the major behavioural modes of consumers are adequately represented in consumers' RLSs. Meanwhile, the weighting of the WSMD set distance ensures that if a single behavioural mode has been split across two or more clusters, that this won't have a significant effect on the pairwise consumer dissimilarities (as demonstrated in Section 5.3). While this incurs minor additional computational complexity, we consider this acceptable given that RVI-based optimisation of each  $k_i$  would require generating more partitions with different numbers of clusters. Initial experimentation suggested that automated RVI optimisation for DLP clustering can show a tendency towards the extremes of the considered range — either oversimplified clusterings ( $k_i = 2$ ) or

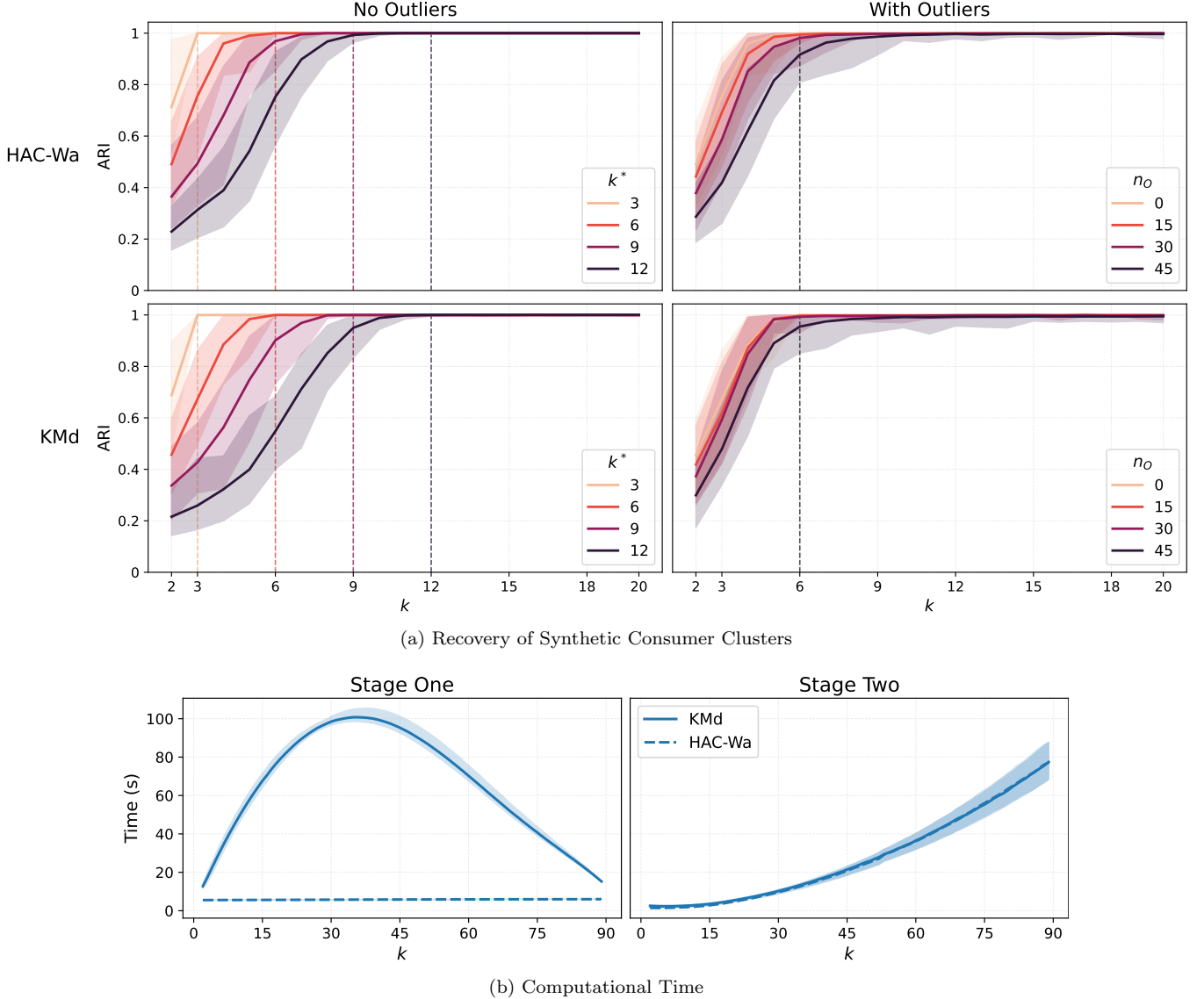


Figure 4: Mean performance and computational time (with pointwise 95 percentile intervals) of the CROCS framework over synthetic datasets with different numbers of true stage one clusters ( $k^*$ ) and different numbers of outliers ( $n_O$ ). (a) Recovery of consumer cluster labels according to ARI for HAC-Wa and KMD with different numbers of stage one clusters ( $k$ ). (b) Computational time (in seconds) for both Stages of the CROCS framework.

excessive partitioning ( $k_i \simeq p_i$ ) — rather than identifying the intermediate value that best captures the behavioural range, a limitation also noted for certain criteria in early comparative evaluations [70].

To demonstrate the utility of overestimation, we applied CROCS to synthetic datasets containing  $m = 300$  consumers with  $p_i = 90$  days of data each, emulating a season’s worth of consumption data. Consumers were distributed among  $K^* = 8$  clusters, with each consumer’s 90 DLPs randomly sampled from their cluster’s unique subset of DLP shapes. Two complementary synthetic data scenarios were considered: one without outlier DLPs and values of  $k^* \in \{2, 3, \dots, 12\}$ , and another where  $k^*$  was fixed at 6 and  $n_O \in \{0, 5, 10, \dots, 80\}$  random DLPs were replaced with outliers. For each of these combinations, 50 independent datasets were generated. In both cases, the data were clustered using the CROCS framework, with the number of stage one clusters systematically varied across  $k \in \{2, 3, \dots, 90\}$ . The true number of consumer clusters,  $K^*$ , was assumed known for the second stage of clustering.

The results from these experiments are presented in Figure 4, with Figure 4a displaying consumer ground-truth label recovery according to ARI<sup>3</sup> when CROCS was applied with either HAC-Wa (top) or KMD (bottom). These experimental results reveal a clear and consistent pattern: overestimating  $k_i^*$  with the same value ( $k$ ) for all consumers provides robust performance without compromising the accuracy of consumer cluster recovery. Once sufficient stage one clusters are extracted to capture each consumer’s behavioural diversity, further increases in  $k$  produce a performance plateau rather than degradation. This finding holds across both experimental scenarios,

<sup>3</sup>Note that the following observations are consistent for both AMI and PSI as well. Also, while only a subset of the described scenarios are shown for clarity in Figure 4a, these observations were consistent across all combinations of  $k^*$  and  $n_O$ .

though the importance of overestimation becomes more pronounced in the presence of outliers.

Without outliers, it was observed to be acceptable to even mildly underestimate  $k^*$  for larger values, likely due to some sharing of the 20 synthetic cluster shapes between consumer clusters — something which is not unlikely in the context of real data. With outliers, there is a greater need for overestimation to ensure accurate recovery of consumer clusters. According to our results with  $k^* = 6$ , even if 50% of DLPs were classified as outliers, using  $2k^*$  would allow acceptable recovery of consumer clusters. For reference, a real consumer DLP dataset was clustered by domain experts in [115] which was composed of 365 DLPs, and it was determined that about 26% of those DLPs should be considered as outliers.

The computational implications of overestimation follow predictable scaling patterns, as shown in Figure 4b. Stage two exhibits quadratic growth in execution time as a function of  $k$ , reflecting the  $\mathcal{O}(k^2)$  pairwise distance computations required between consumer RLSs. Meanwhile, stage one scales with the complexity of the chosen clustering algorithm — the complexity of KMD depends on the choice of  $k^4$ , while the distance matrix and dendrogram computations in HAC-Wa are identical for any  $k$ . Since the stage one clustering operations can be performed independently for each consumer, execution time can be reduced dramatically through parallel implementation. In contrast, stage two performs a single clustering operation across all consumers, making the quadratic scaling in RLS size the dominant computational bottleneck for a given size dataset.

In summary, while overestimating  $k_i$  with a uniform choice of  $k$  seemingly incurs additional computational time, particularly in stage two, these costs represent a reasonable trade-off in light of the simplicity and robustness afforded. The computational overhead remains practical, especially considering that it eliminates the need to select an appropriate set of RVIs, and perform extensive clustering to optimise those RVIs independently for each consumer — a process that would itself be computationally expensive and potentially less reliable.

## 5.2 Comparing Consumer Representations

As discussed in Section 2.3, adequately capturing intra-consumer variation is important for effective consumer clustering, as this variability can serve as an indicator of suitability for DSM strategies. In the CROCS framework, intra-consumer variation is preserved within the RLS in the form of a diverse set of prototypical daily consumption profiles. While the RLS offers comprehensive behavioural representation, it is valuable to consider how it compares to other DLP-based methods from the literature.

As outlined in Section 2.2, several consumer representation methods are also based on processed DLPs. RLPs are the simplest example, relying on simple point-wise averages across all DLPs. DCPs suggested by Tsekouras et al. [103] represent each consumer by the prototype of their most populated cluster from a similar stage one clustering to that in CROCS. In contrast, the GPF approach from Li et al. [57] represents consumers through proportion vectors indicating how frequently their DLPs resemble globally-discovered prototypical DLPs. Unlike the rigid RLP, the representational quality and efficiency of the RLS, DCP, and GPF are particularly dependent upon the number of stage one clusters ( $k$ ) used to generate them.

To evaluate how effectively each representation captures intra-consumer variability, we computed the reconstruction error (using ED) between real consumer’s DLPs and their closest representative profile. For the RLP and DCP representations, which provide only a single representative profile per consumer, all DLPs were compared against this single profile. For the RLS and GPF representations, which rely upon multiple profiles, each DLP was compared against its closest profile from the available set. Given that this concept of reconstruction error aligns with the objective function of  $k$ -means (within-cluster sum of squares), we have used  $k$ -means with ED to generate the RLS, DCP, and GPF representations for this comparison<sup>5</sup>.

Figure 5 displays the mean reconstruction error across all consumers for values of  $k \in \{2, 3, \dots, 80\}$ . The left panel shows results for the AG dataset, averaged across 24 different 90-day periods (one starting on the first day of each month in 2011 and 2012), while the right panel shows results for the SGSC dataset averaged across 10 90-day periods (one starting on the first day of each of the first 10 months of 2013).

Clearly, the multiple profiles in the RLS and GPF representations offer a significant advantage over the single profile representations. In particular, the single DCP exhibits a higher reconstruction error for all  $k$  than even the simple RLP. The quality of the DCP representation in fact deteriorates as  $k$  is increased. This deterioration occurs because as  $k$  increases, each consumer’s DLPs are distributed across more clusters, causing the most populated cluster to represent a progressively smaller fraction of the consumer’s behaviour. Figure 6 demonstrates this effect using the same datasets as Figure 5, showing the proportion of DLPs assigned to each consumer’s largest cluster for different values of  $k$ . This particular analysis used DTW-2 distance with both HAC-Wa and KMD algorithms, with results aggregated across both clustering methods and all AG and SGSC datasets due to the consistency of the trend. The mean proportion only marginally exceeds what would be expected under uniform random partitioning into  $k$  groups, following a similar declining trend as  $k$  increases. By the time  $k$  reaches 3, the largest cluster represents only about

<sup>4</sup>For KMD, the algorithm’s update step evaluates  $k(p_i - k)$  possible medoid swaps, which is smallest when  $k$  is near the extremes and largest when  $k$  is intermediate, resulting in the observed peak in execution time.

<sup>5</sup>Though similar results were found when using KMD and HAC-Wa with either ED or DTW-2, and either mean or medoid prototypes.

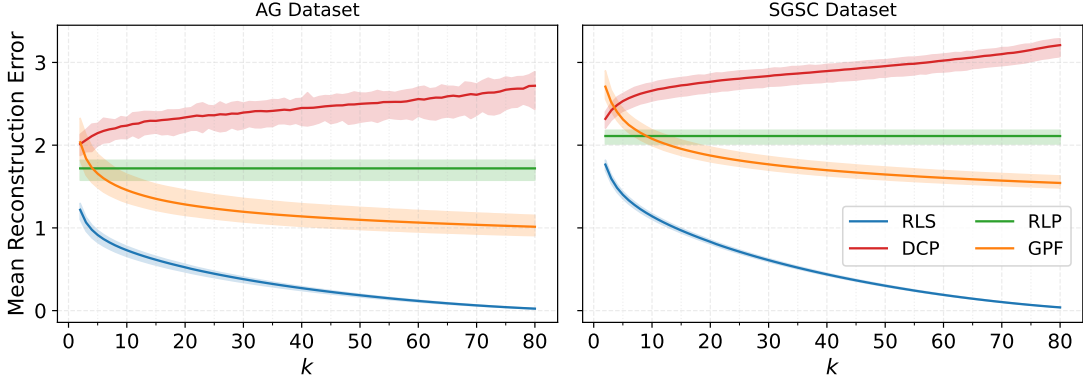


Figure 5: Mean reconstruction error (according to ED) for different load-profile based consumer representation methods across varying numbers of stage one clusters ( $k$ ). Results are averaged across consumers and multiple 90-day periods: 24 periods for the AG dataset (left) and 10 periods for the SGSC dataset (right). Shaded regions show the full range of variation across the different time periods.

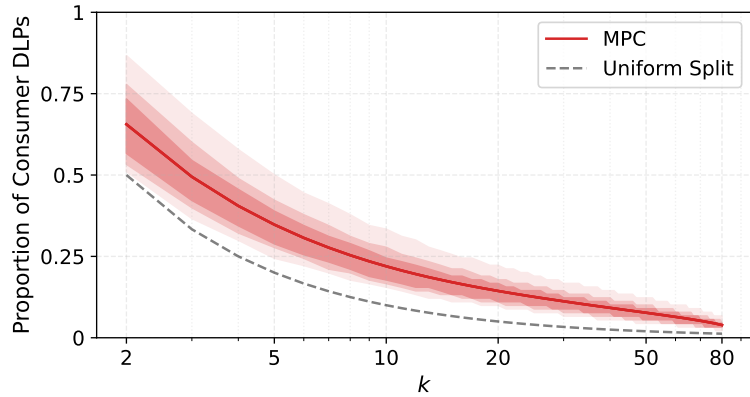


Figure 6: Proportion of DLPs appointed to the largest cluster across different values of  $k$  (displayed on a log-scale). The red line shows the mean proportion, with shaded regions representing the central 50%, 70%, and 90% intervals of the distribution. Results are based on all consumers from the AG and SGSC datasets over the same 90 day periods behind Figure 5, but clustered using DTW-2 with either HAC-Wa or KMd algorithms to achieve more representative partitions. The grey dashed line indicates the expected proportion under uniform cluster size distribution for comparison.

half of the DLPs — not to mention that such a clustering is very unlikely to adequately segment a consumer’s DLPs across their true set of behavioural modes.

Unlike DCP, the reconstruction error for RLS and GPF decreases steadily as  $k$  increases, approaching zero at the limits of  $p$  and  $mp$ , respectively. However, comparing them directly at the same  $k$  is not straightforward as RLS uses  $k$  local prototypes per consumer (totalling  $mk$ ), whereas GPF uses  $k$  global prototypes shared across all consumers. In principle, with sufficiently large  $k \gg p$ , GPF could achieve the same reconstruction error of RLS. In practice, however, GPF has typically been applied with small  $k$  values. For instance, Li et al. [57] used  $k \in \{2, \dots, 10\}$  for  $m = 1463$  vehicles over one year, while Nakashima et al. [75] used  $k \in \{30, 50, 100\}$  for datasets with  $mp$  on the order of  $10^4$ . This preference for modest  $k$  stems from both computational and statistical issues. As  $k$  increases, the dimensionality of the frequency vectors grows, causing the distances between them to become increasingly concentrated, thereby reducing their discriminative power [2]. At the same time, meaningful behavioural modes risk being fragmented across multiple clusters, so that subtle similarities between consumers are obscured when their counts are split across distinct dimensions. These factors constrain GPF’s practical effectiveness, making comparisons with  $k \in \{2, \dots, 80\}$  more representative of practical usage. Within this range, the localised RLS approach consistently provides lower reconstruction error, highlighting its advantage over global representations for efficiently capturing intra-consumer variability.

Despite the practical restrictions of applying GPF with large  $k$  in practice, it is insightful to examine the relationship between the number of clusters required by GPF and RLS to achieve identical reconstruction errors. Figure 7 shows the values of  $k_{\text{GPF}}$  (y-axis) and  $k_{\text{RLS}}$  (x-axis) that produce equivalent reconstruction errors for the AG datasets analysed in Figure 5. Linear spline interpolation was used to determine these equivalent cluster numbers across different starting months.

The results reveal significant redundancy in the RLS representation. For instance, when  $k_{\text{RLS}} = 5$ , there are effectively 1500 local representative profiles for the AG consumers, yet the GPF representation suggests that only

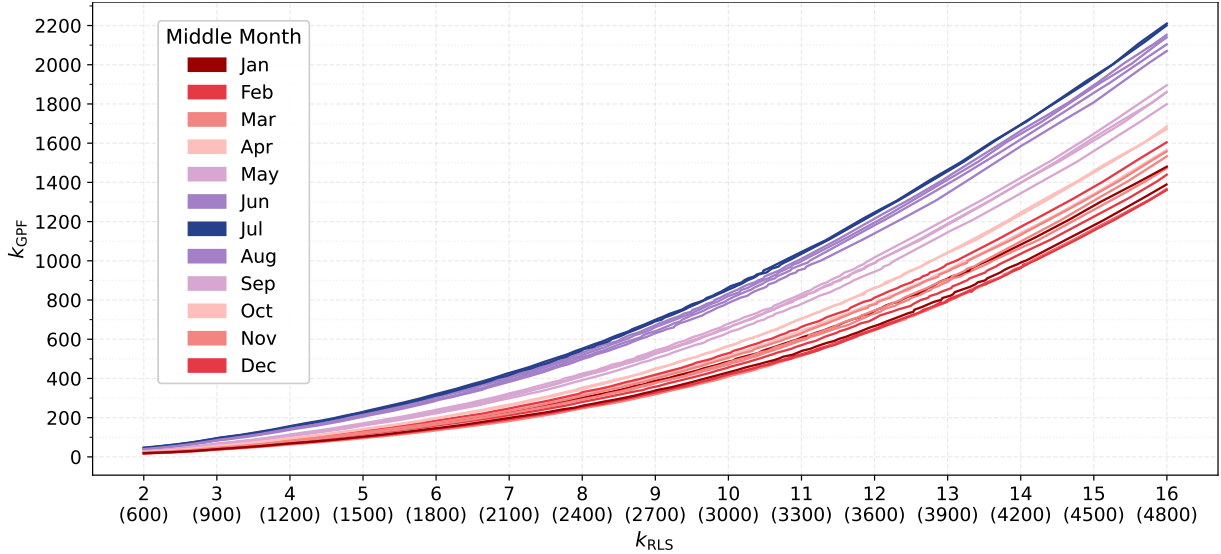


Figure 7: Values of  $k_{\text{GPF}}$  (y-axis) and  $k_{\text{RLS}}$  (x-axis) for the GPF and RLS representations respectively that achieve identical reconstruction errors across the 24 90-day periods from the AG dataset. Both representations have been computed using ED and  $k$ -means. Line shading reflects the climate of the midpoint month, with a palette mirrored around January and July to emphasise seasonal trends in the relationship between equivalent  $k_{\text{GPF}}$  and  $k_{\text{RLS}}$ . Values of  $k_{\text{RLS}}$  are provided on the x-axis with the effective number of representative profiles across all consumers in brackets underneath ( $m \times k_{\text{RLS}}$ ).

100-200 global representative profiles would achieve the same reconstruction error. Interestingly, seasonal variation in this redundancy is also evident from the colour-coded lines in Figure 7. Again for  $k_{\text{RLS}} = 5$ , approximately 100 global profiles provide equivalent reconstruction error during summer months, while over 200 are required during winter. This pattern suggests greater diversity in consumption behaviours during cooler months, potentially due to variability among households in terms of insulation quality, heating systems, temperature tolerance, and other demographic factors.

Rather than representing a limitation, this redundancy in the RLS representation supports the premise that consumers exhibit similar energy usage patterns, validating the potential effectiveness of consumer clustering. The CROCS framework leverages this redundancy to group consumers based on their shared behaviours.

### Computational Complexity

While the RLS representation involves more individual representative profiles than the GPF representation, it offers considerable computational advantages. Consider RLS, where each of  $m$  consumers'  $p$  DLPs are independently clustered using HAC-Wa<sup>6</sup>, resulting in a complexity of  $\mathcal{O}(mp^2)$ . GPF meanwhile clusters all  $mp$  DLPs together, at a complexity of  $\mathcal{O}(m^2p^2)$ , scaling poorly with the number of consumers in the dataset. When combined with the second stage of clustering, involving  $k^2$  WSMD distance computations for each consumer pair, the complexity of the CROCS framework is  $\mathcal{O}(mp^2 + k^2m^2)$ . Meanwhile, using the GPF for consumer clustering collectively achieves a complexity of  $\mathcal{O}(m^2p^2 + km^2)$ . The squared dependence on  $m$  in GPF's first stage is traded for a linear dependence on  $m$  in CROCS' first stage, while the linear dependence on  $k$  in GPF's second stage becomes quadratic in CROCS. Since  $k \ll m$  in practice, this trade-off represents a substantial computational advantage for CROCS, making consumer clustering feasible at scales where GPF approaches would become computationally intractable. Moreover, CROCS also benefits further from straightforward parallelisation across consumers in its first stage.

### 5.3 Stage Two: Is WSMD the best Set Distance Measure?

WSMD was designed specifically for comparing consumer RLSs. However, any set-to-set distance could in principle be employed in Stage Two of CROCS instead. To demonstrate the advantages of WSMD, we conducted a comparative evaluation against a broad set of alternatives using synthetic datasets.

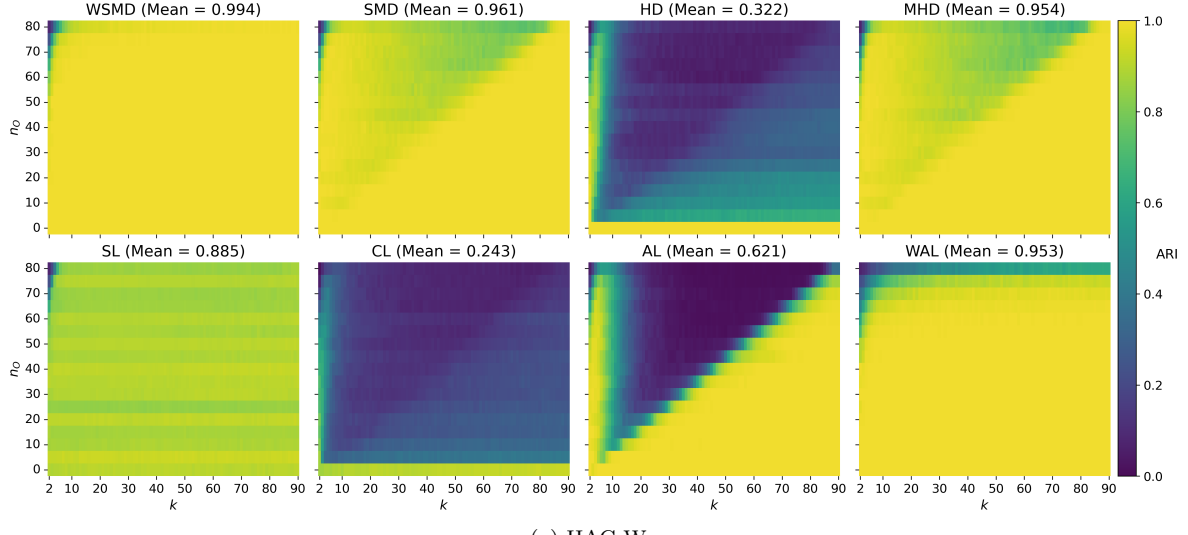
In this case, the synthetic datasets contained 50 consumers with 90 days of data each, distributed among  $K^* = 2$  clusters, with cluster sizes again determined by a multinomial distribution with uniform probabilities. These two clusters were defined by distinct pairs of DLP shapes randomly sampled from the available 20. One hundred such datasets were generated for each  $n_O \in \{0, 5, 10, \dots, 80\}$ .

The consumers were clustered using CROCS with the number of stage one clusters systematically varied across  $k \in \{2, 3, \dots, 90\}$ , using the default configuration. For the second stage of clustering,  $K^*$  was assumed known, and 8

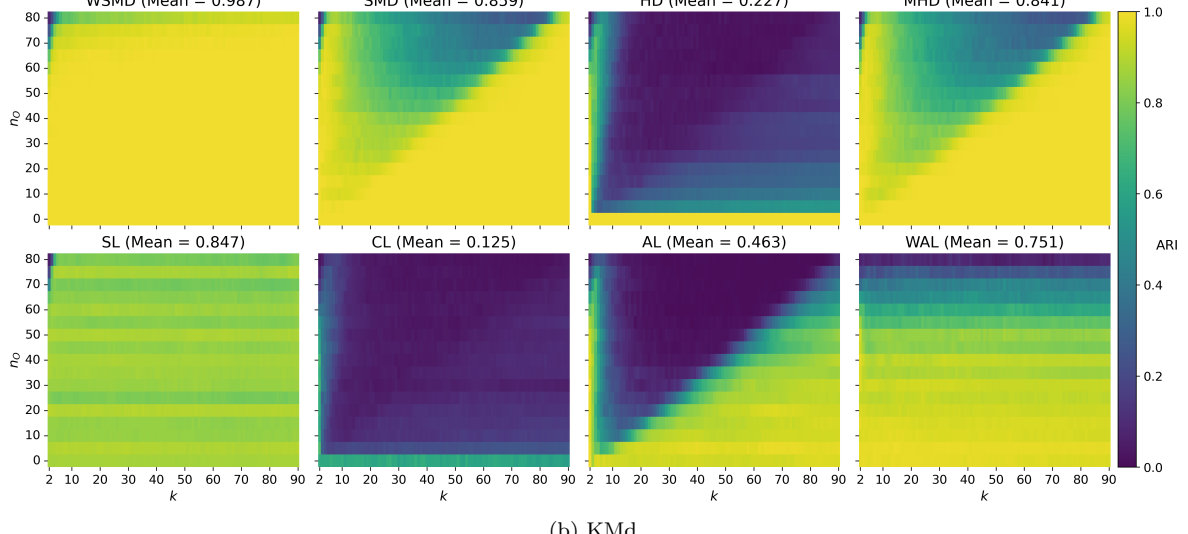
<sup>6</sup>Which has complexity  $\mathcal{O}(n^2)$  for  $n$  objects [74].

Set Distance	Acronym	Equation
Weighted Sum of Minimum Distances	WSMD	$\Delta_{\text{WSMD}}(\hat{\mathcal{S}}_i, \hat{\mathcal{S}}_j) = \frac{1}{2} \left[ \frac{1}{p_i} \sum_{a=1}^{k_i} n_i^a \min_b d(\boldsymbol{\pi}_i^a, \boldsymbol{\pi}_j^b) + \frac{1}{p_j} \sum_{b=1}^{k_j} n_j^b \min_a d(\boldsymbol{\pi}_j^b, \boldsymbol{\pi}_i^a) \right]$
Sum of Minimum Distances	SMD	$\Delta_{\text{SMD}}(\hat{\mathcal{S}}_i, \hat{\mathcal{S}}_j) = \frac{1}{2} \left[ \sum_{a=1}^{k_i} \min_b d(\boldsymbol{\pi}_i^a, \boldsymbol{\pi}_j^b) + \sum_{b=1}^{k_j} \min_a d(\boldsymbol{\pi}_j^b, \boldsymbol{\pi}_i^a) \right]$
Hausdorff Distance	HD	$\Delta_{\text{HD}}(\hat{\mathcal{S}}_i, \hat{\mathcal{S}}_j) = \max \left\{ \max_a \min_b d(\boldsymbol{\pi}_i^a, \boldsymbol{\pi}_j^b), \max_b \min_a d(\boldsymbol{\pi}_j^b, \boldsymbol{\pi}_i^a) \right\}$
Modified Hausdorff Distance	MHD	$\Delta_{\text{MHD}}(\hat{\mathcal{S}}_i, \hat{\mathcal{S}}_j) = \max \left\{ \frac{1}{k_i} \sum_{a=1}^{k_i} \min_b d(\boldsymbol{\pi}_i^a, \boldsymbol{\pi}_j^b), \frac{1}{k_j} \sum_{b=1}^{k_j} \min_a d(\boldsymbol{\pi}_j^b, \boldsymbol{\pi}_i^a) \right\}$
Single Linkage	SL	$\Delta_{\text{SL}}(\hat{\mathcal{S}}_i, \hat{\mathcal{S}}_j) = \min_a \min_b d(\boldsymbol{\pi}_i^a, \boldsymbol{\pi}_j^b)$
Complete Linkage	CL	$\Delta_{\text{CL}}(\hat{\mathcal{S}}_i, \hat{\mathcal{S}}_j) = \max_a \max_b d(\boldsymbol{\pi}_i^a, \boldsymbol{\pi}_j^b)$
Average Linkage	AL	$\Delta_{\text{AL}}(\hat{\mathcal{S}}_i, \hat{\mathcal{S}}_j) = \frac{1}{k_i k_j} \sum_{a=1}^{k_i} \sum_{b=1}^{k_j} d(\boldsymbol{\pi}_i^a, \boldsymbol{\pi}_j^b)$
Weighted Average Linkage	WAL	$\Delta_{\text{WAL}}(\hat{\mathcal{S}}_i, \hat{\mathcal{S}}_j) = \frac{1}{p_i p_j} \sum_{a=1}^{k_i} \sum_{b=1}^{k_j} n_i^a n_j^b d(\boldsymbol{\pi}_i^a, \boldsymbol{\pi}_j^b)$

Table 3: Set distances compared for stage two of the CROCS framework. Note that  $\mathcal{S}_i$  is the  $i^{\text{th}}$  consumer's RLS, which contains  $k_i$  prototypical DLPs. The  $a^{\text{th}}$  such prototype is  $\boldsymbol{\pi}_i^a$ , which represents  $n_i^a$  of the consumers  $p_i$  total DLPs. Furthermore, note that  $d(\cdot, \cdot)$  is a time series dissimilarity measure.



(a) HAC-Wa



(b) KMd

Figure 8: Heatmaps of mean ARI values, indicating synthetic consumer cluster recovery when utilising different set distances to compute dissimilarity between consumer RLSs in stage two of the CROCS framework. In a) and b), the HAC-Wa and KMd clustering algorithms were used respectively. The average ARI across all numbers of outliers ( $n_O$ ) and numbers of stage one clusters ( $k$ ) is also provided.

set distances (detailed in Table 3) were employed to compare their suitability in recovering consumer clusters. Among these 8 are familiar set distances such as the Hausdorff distance [96], and others commonly used in agglomerative hierarchical clustering such as single, complete, and average linkage [3]. We also considered the original unweighted version of the WSMD (the sum of minimum distances), a version of the Hausdorff distance designed to emulate WSMD by replacing the first maximum operation with a mean, and a version of average linkage with pairwise distances weighted by the product of their respective cluster sizes.

The results from this experiment according to the ARI are presented in Figure 8, with HAC-Wa and KMd used as the clustering algorithm in Figures 8a and 8b respectively. Note that these results were consistent with AMI and PSI.

For both HAC-Wa and KMd, the proposed WSMD consistently obtained the largest ARI values out of all considered set distances, indicating better recovery of the consumer clusters. As recognised in Section 5.1, recovery of consumer cluster labels naturally becomes more difficult when more outliers are introduced. WSMD showed the greatest robustness to an increase in the number of outlier DLPs, only showing difficulties at extreme values, i.e.  $n_O \geq 70$ . Meanwhile, the closest competitor methods, SMD and MHD, were both affected by the increased proportion of outliers when overestimating  $k$ . As these set distances both place equal significance on all pairwise distances between RLS prototypes, when outliers are increasingly represented in the RLS, consumer similarity can be obscured. Furthermore, for SMD and MHD, perfect label recovery could be achieved for large values of  $k$  that grow linearly with  $n_O$ , yet WSMD required the smallest overestimation to reliably discover the same consumer clusters. This robustness is desirable when the true  $n_O$  is unknown in real datasets. This experiment provides assurance that WSMD is well-suited to computing pairwise dissimilarities between consumer RLSs.

## 5.4 Identifying Similar Consumers on Asynchronous Schedules

As discussed in Section 2.3, many existing clustering approaches rely on temporally anchored comparisons, which can cause households with highly similar daily consumption patterns expressed on different days to be assigned to different clusters. This undermines the effectiveness of segmentation for downstream applications, where the similarity of underlying patterns often matters more than their alignment on the calendar. For example, two households with comparable routines but staggered work schedules may be equally well suited to the same tariff.

To demonstrate different forms of consumer relationships present in real data, we examine archetypal pairs of consumers drawn from the AG dataset. In Figure 9, each panel shows the daily cluster assignments of two consumers over a six-month period. Each dot corresponds to one consumer's DLP, positioned by day and cluster label on the horizontal and vertical axes respectively. Blue and orange dots mark the cluster memberships of the individual consumers, and green dots highlight days when both consumers' DLPs were assigned to the same cluster. The DLPs of the consumer pairs were clustered together into 10 clusters using min-max normalisation, DTW-2 and HAC-Wa. We provide *two* examples for *each* of three archetypal consumer relationships. In the top row are two consumer pairs whose DLPs did not share any clusters over the 6 month period, indicating fundamentally distinct consumption behaviours. In contrast, the middle and bottom rows show pairs of consumers whose DLPs were assigned to the same clusters, indicating shared consumption behaviours. In the middle row, these shared behaviours are temporally aligned, while in the bottom row, they occur asynchronously. Including two examples per archetype illustrates the diversity within each category, with differences in how similarity and alignment manifest. Ten clusters were sought to allow unique consumption behaviours to be adequately captured in their own clusters, while avoiding excessive fragmentation that could emphasise noise rather than meaningful behavioural differences.

The archetypal examples in Figure 9 define the extremes of consumer relationships, with most other consumers falling somewhere between these reference points. These relationships can be quantified using two complementary metrics. Firstly, similarity between behavioural distributions for a pair of consumers can be measured using the normalised Jensen-Shannon Divergence (JSD) [59] between cluster membership counts. The normalised JSD is symmetric, and bounded between 0 and 1 for discrete probability distributions, with *lower values indicating greater overlap in consumer behaviours*. Secondly, the temporal alignment of those cluster sequences can be measured using normalised Cohen's  $\kappa$  [29], which accounts for the possibility of alignment due to chance. The normalised  $\kappa$  ranges between 0 and 1, with values around 0.5 and lower indicating agreement by chance alone, and values approaching 1 indicating perfect agreement.

Consumers with similar behavioural distributions that are not temporally aligned will have cluster sequences that produce low values of JSD, and  $\kappa$  around 0.5. To understand how common these consumers are in a real-world dataset, we computed these two metrics for all consumer pairs in the AG dataset across multiple time periods. Figure 10 provides a density-shaded scatterplot of JSD and  $\kappa$  for all  $\binom{300}{2}$  consumer pairs across 24 six-month periods starting in each month of 2011 and 2012. The six consumer pairs in Figure 9 are located within the plot with colour-coded markers for reference.

The densest region of the scatterplot in Figure 10 is at  $(1.0, 0.5)$ , where consumer pairs have distinct behavioural distributions and, resultingly, no temporal alignment of their consumption behaviours. This is expected because each consumer can be paired with far more households that do not share its behaviours than those that do. However,

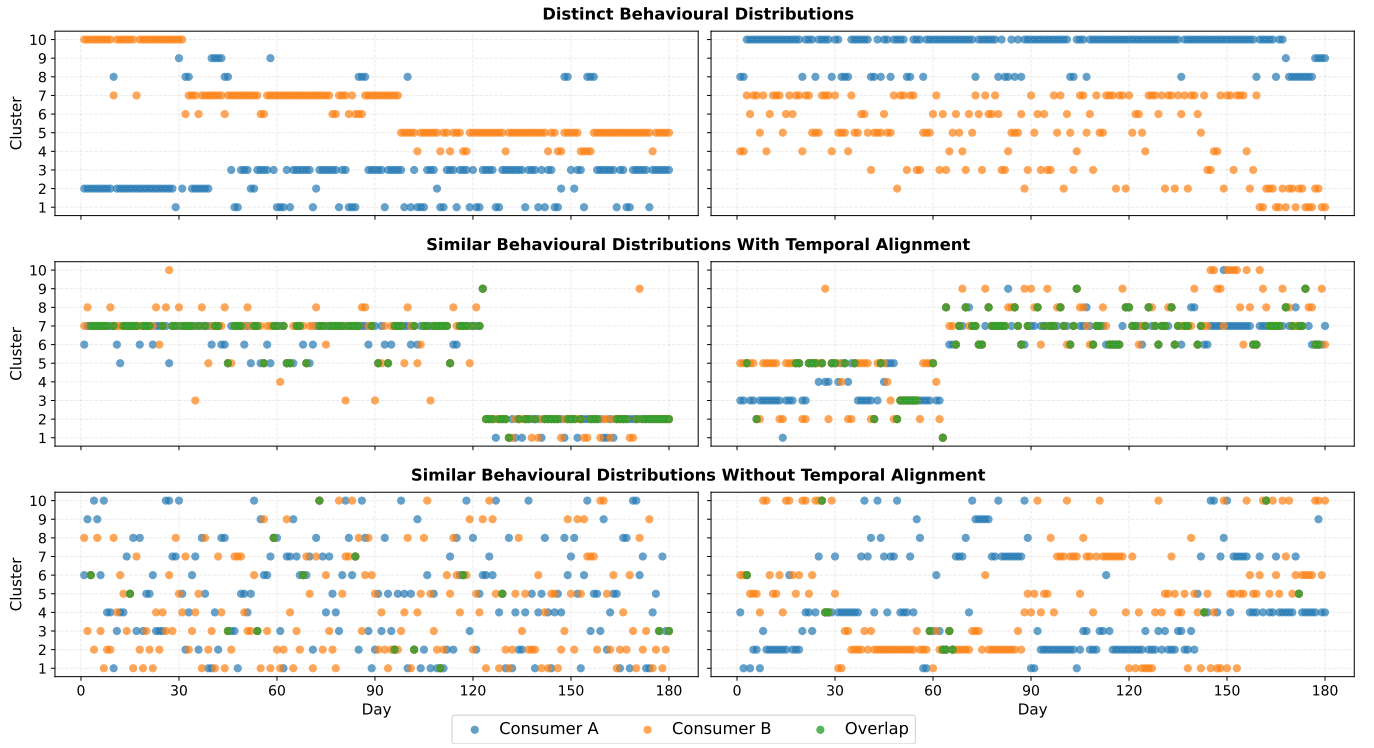


Figure 9: Temporal evolution of cluster membership for archetypal consumer pairs from the AG dataset. For each archetypal, two example pairs (left and right) are shown to illustrate some within-category diversity. The 360 DLPs of these consumer pairs (from 6 months of consumption data) have been clustered into 10 clusters. Blue and orange markers indicate the respective cluster membership of the consumers' DLPs, with green indicating days with identical membership. The archetypal pairs include: (Top) Consumers with distinct behavioural distributions; (Middle) Consumers with similar behavioural distributions with temporal alignment; (Bottom) Consumers with similar behavioural distributions without temporal alignment.

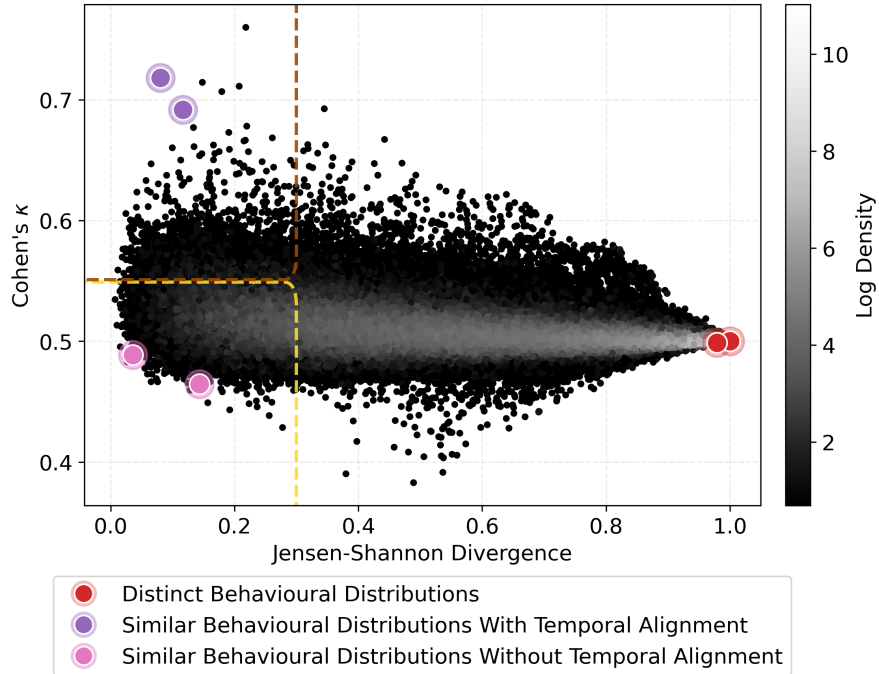


Figure 10: Log-density shaded scatterplot of JSD and Cohen's  $\kappa$  computed for all pairs of AG consumers over 24 six-month periods starting in each month of 2011 and 2012. Each consumer pair's 360 DLPs were clustered together into 10 clusters. JSD and  $\kappa$  were then computed between the resulting sequences. The bottom left region enclosed by the yellow dashed line ( $\kappa < 0.55$ ,  $JSD \leq 0.3$ ) indicates pairs of consumers that share similar behavioural distributions, with low temporal alignment. The upper left region enclosed by the brown dashed line ( $\kappa > 0.55$ ,  $JSD \leq 0.3$ ) indicates pairs that share similar distributions, with higher temporal alignment.

a notable proportion of consumer pairs fall into the bottom left region of the scatterplot, bordered by the yellow dashed line, where they exhibit substantial overlap in their consumption behaviours but at different times. For indicative purposes, around 7.7% of pairs fall into this region ( $\kappa < 0.55$ ,  $JSD \leq 0.3$ ), compared with only 0.6% in the brown region ( $\kappa > 0.55$ ,  $JSD \leq 0.3$ ) where similar behaviours are more strongly aligned. The consumer pairs shown in the middle row of Figure 9 with temporal alignment (purple markers in the upper left of Figure 10) are at the extreme upper end of  $\kappa$ 's range, with  $\kappa \approx 0.7$ . The majority of consumers however have  $\kappa$  values well below this (typically  $< 0.6$ ), indicating that strong behavioural *and* temporal alignment is exceedingly rare. While the specific percentages of pairs in these regions depend on the chosen thresholds, the large disparity indicated here illustrates that asynchronous similarity is likely much more common than temporally aligned similarity. As a result, many existing approaches that rely on calendar synchronisation are likely to miss a substantial share of functionally similar consumers.

#### 5.4.1 Comparative Analysis

Having demonstrated that consumers with asynchronous similarity are more abundant in real-world data than those with synchronised similar behaviours, we next evaluated how well existing clustering methods could identify such asynchronous similarity. To enable a controlled comparison, we conducted a synthetic data experiment where the ground truth consumer relationships were known. We begin by describing the process used to generate the synthetic data for this experiment.

As in previous synthetic experiments, clusters of consumers shared the same  $k^*$  synthetic DLP shapes. However, to create more realistic consumption time series for methods that compute features from or operate directly on long time series, we determined each consumer's sequence of shapes by generating random sequences from first-order Markov models fitted to real-world consumer shape sequences. We first validated that first-order Markov models appropriately characterise the day-to-day evolution of consumption patterns for real consumers using Csiszar's  $\phi$ -divergences for testing Markov process order [65].

Clustering Algorithm	Dataset	
	AG	SGSC
HAC-Wa	0.999	0.948
KMd	0.996	0.926

Table 4: Proportion (to 3 significant figures) of consumer cluster membership sequences identified as first order Markovian according to Csiszar's order test at the 0.05 significance level. Sequences were obtained for consumers individually with DTW-2 and either HAC-Wa or KMd clustering algorithms on the AG and SGSC datasets.

Table 4 shows the proportion of AG and SGSC consumers with cluster label sequences that demonstrate a first-order Markovian relationship for  $k \in \{2, 3, \dots, 50\}$ . The DLP clustering for each consumer was performed using DTW-2 on min-max normalised profiles with either HAC-Wa or KMd. In Csiszar's order test, the null hypothesis states that the sequence is random, while the alternative posits that it follows a first-order Markov process, where transition probabilities only depend on the current state. We analysed the 300 AG consumer sequences with the full 1096 days each, spanning 01/07/2010 to 30/06/2013<sup>7</sup>, and the 3953 SGSC sequences with the full 365 days each, covering all of 2013. The vast majority of consumers were well-fitted by a first-order Markov process. Even with highly conservative Bonferroni corrections accounting for all 49 values of  $k$  and all consumers, the proportions remained high: 0.989 (HAC-Wa) and 0.986 (KMd) for AG consumers, and 0.737 (HAC-Wa) and 0.676 (KMd) for SGSC consumers.

Since the AG dataset provided more historical data for reliable estimation of Transition Probability Matrices (TPMs), we used it as the basis for synthetic data generation, restricted to those consumers whose cluster sequences exhibited Markovian behaviour across all  $k \in \{2, 3, \dots, 50\}$  for both HAC-Wa and KMd. To generate synthetic data for a consumer cluster with  $k^*$  distinct consumption patterns, we randomly selected one TPM estimated from the real-world AG clustering results with  $k = k^*$  clusters. All synthetic consumers within the same cluster shared both the same  $k^*$  synthetic consumption patterns and the same TPM, but each consumer's pattern sequence was independently sampled from this TPM. This approach encourages the synthetic time series to reflect a realistic evolution of daily patterns for the target number of clusters, while maintaining behavioural cohesion within consumer clusters.

The resulting temporal alignment of consumer pattern sequences from this generation process are shown in Figure 11, where histograms record the proportion of days with identical cluster membership among 1000 90-day sequences sampled from 8 different TPMs trained on consumers from the AG dataset. The key takeaway is that for smaller values of  $k^*$ , synthetic consumers in the same cluster could have low or high temporal alignment, while for larger values, lower temporal alignment is the norm.

<sup>7</sup>Using the dd/mm/yyyy format.

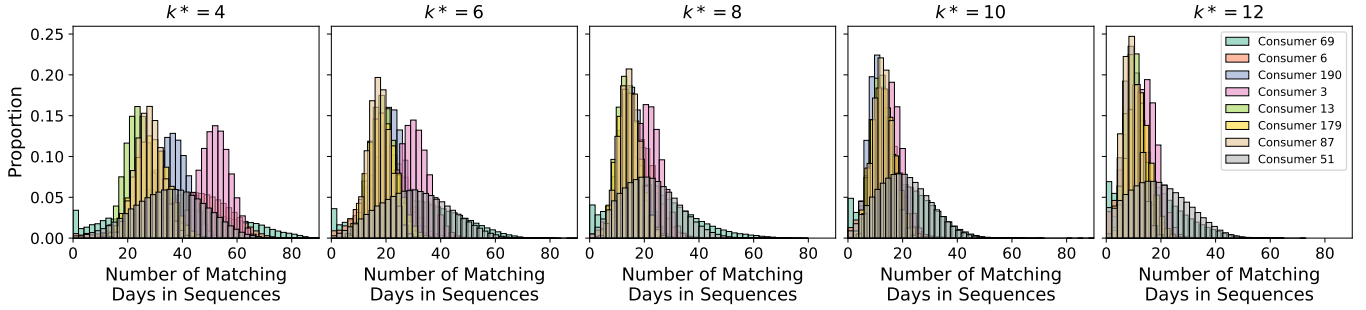


Figure 11: Histograms showing the proportion of days with identical cluster membership for consumer pairs within the same synthetic cluster. Sequences were generated for 8 random TPMs trained on real AG consumer cluster label sequences that were validated as first-order Markovian by Csiszar’s test for all  $k \in \{4, 6, 8, 10, 12\}$ . Each histogram is based on 1000 synthetic sequences, spanning 90 days generated from each consumer’s TPM.

The synthetic datasets used for this experiment were generated with 300 consumers, split into  $K^* = 8$  clusters, with  $k^* \in \{4, 6, 8, 10, 12\}$  distinct synthetic DLP shapes. A total of  $n_O \in \{0, 20, 40, 60\}$  DLPs from the 90 day sequences were replaced with outlier DLPs. Furthermore,  $N_O \in \{0, 50, 100\}$  consumers from the 300 were designated as outlier consumers. These outlier consumers had their own distinct set of  $k^*$  DLP shapes, and their own distinct TPM for generating shape sequences. These outlying consumers were intended to obscure the otherwise well-separated consumer clusters, but recognition of their outlier status was not pertinent to our experiment. As such, when computing the EVIs, the labels of these consumers were ignored. Ten datasets were generated for each combination of settings.

To benchmark the capacity of CROCS to discover asynchronous consumer similarity, we selected a broad range of representative methods from the consumer clustering literature. These methods fall into two main categories: single-stage clustering approaches and two-stage clustering approaches. The single-stage methods include the following representations: RLPs, normalised Long Time Series (LTS), Autocorrelation (ACF) and Partial Autocorrelation features (PACF), Delay Coordinate Embedding (DCE) map parameters as in [73], and Discrete Wavelet Transform (DWT) coefficients. Each representation was applied to the data using multiple clustering algorithms, and with multiple parameter settings where appropriate. All representations were paired with  $k$ -means, HAC-Wa and KMD using ED. RLPs and LTS were additionally applied using DTW-2. As for [8], the ACF and PACF were computed using 96 lags. DCE map parameters were found for embedding dimensions  $m$ , and delay  $\tau \in \{5, 10, 15, 20, 25, 30\}$ . Furthermore, instead of applying a linear neural regression to obtain the map parameters, the analytical solution was used. Finally, for DWT we considered the Haar and Coiflet-8 mother wavelets (as in [104]) at all possible levels of decomposition, using either all coefficients, just the approximation coefficients, or the last pair of detail and approximation coefficients. For a best-case comparison with CROCS, the combination of parameters, clustering algorithm and distance measure that produced the highest average ARI with each representation is the version for which results are presented.

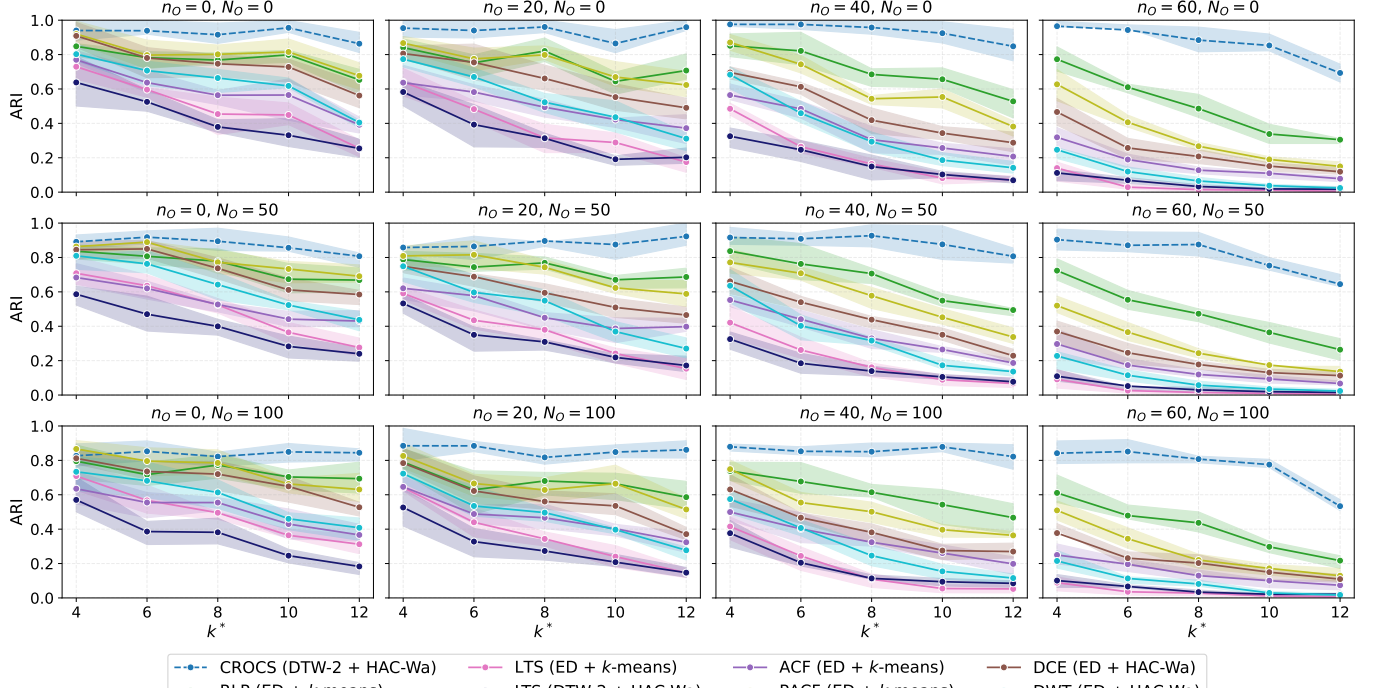
Meanwhile, the two-stage methods include the following: GPFs and DCPs with DTW-2 and either HAC-Wa or KMD, and the Daily Ensemble method as implemented by Sun et al. [95], where  $k$ -means was applied independently on each day’s DLPs in the first stage followed by spectral clustering of a similarity matrix indicating how frequently households were grouped together in the second stage. These methods are united with CROCS by the parameter  $k$ , that is, the number of clusters used in the first stage of clustering. For all methods, we clustered the datasets with  $k \in \{2, 3, \dots, 80\}$ . Figure 12 summarises the results according to the ARI from these experiments, with single- and two-stage methods compared with CROCS in Figure 12a and Figure 12b respectively.

In Figure 12a, the mean ARI values are plotted with a 50 percentile interval for each  $k^*$ , with columns containing results for datasets with different numbers of DLP outliers ( $n_O$ ), and rows containing results for datasets with different numbers of outlying consumers ( $N_O$ ). The performance of CROCS when  $k = 15$  is shown with a dashed line for comparison. CROCS was found more capable of recognising asynchronous similarity than all of the other single-stage methods, regardless of  $k^*$  or the number of each kind of outlier. CROCS is also the least affected by  $k^*$ , with most other methods showing a more precipitous drop in mean ARI with increasing  $k^*$ . This collective drop in performance is likely related to the previous observation from Figure 11 that as  $k^*$  increases, our synthetic consumers show much lower temporal alignment of their common consumption patterns. Interestingly, the simple RLP appears to be the next best method after CROCS, likely due also to its independence from the ordering of consumer DLPs. Clustering approaches that use the normalised LTS performed the worst — especially for the largest values of  $n_O$  — likely due to the combination of asynchronous similarity and the curse of dimensionality.

Due to sharing the important and comparable parameter  $k$ , for the two-stage methods we have instead provided results for  $k^* = 8$  in Figure 12b, with the  $x$ -axis instead showing variation in performance for different values of  $k$ . However, plots for  $k^* \in \{4, 6, 10, 12\}$  provided consistent observations. The rows and columns still mirror those of

Figure 12a. This time we can see that there is less separation between CROCS and the next best performer in GPF, especially for lower  $n_O$ . However, as  $n_O$  increases, the GPF representation requires much larger values of  $k$ , relative to CROCS, to account for the additional outlying shapes in the datasets. Meanwhile, the daily ensemble method also struggles considerably with increasing values of  $n_O$  as consumers exhibit shapes on more days that are not aligned with the core shapes of their ground truth cluster. The DCP performs poorly in all scenarios, as consumers' most common consumption profiles will not always be shared with the other consumers in their cluster due to the random sampling of pattern sequences from their shared TPMs.

These results demonstrate that CROCS consistently outperforms both single-stage and two-stage clustering meth-



(a) Single-Stage Methods vs CROCS

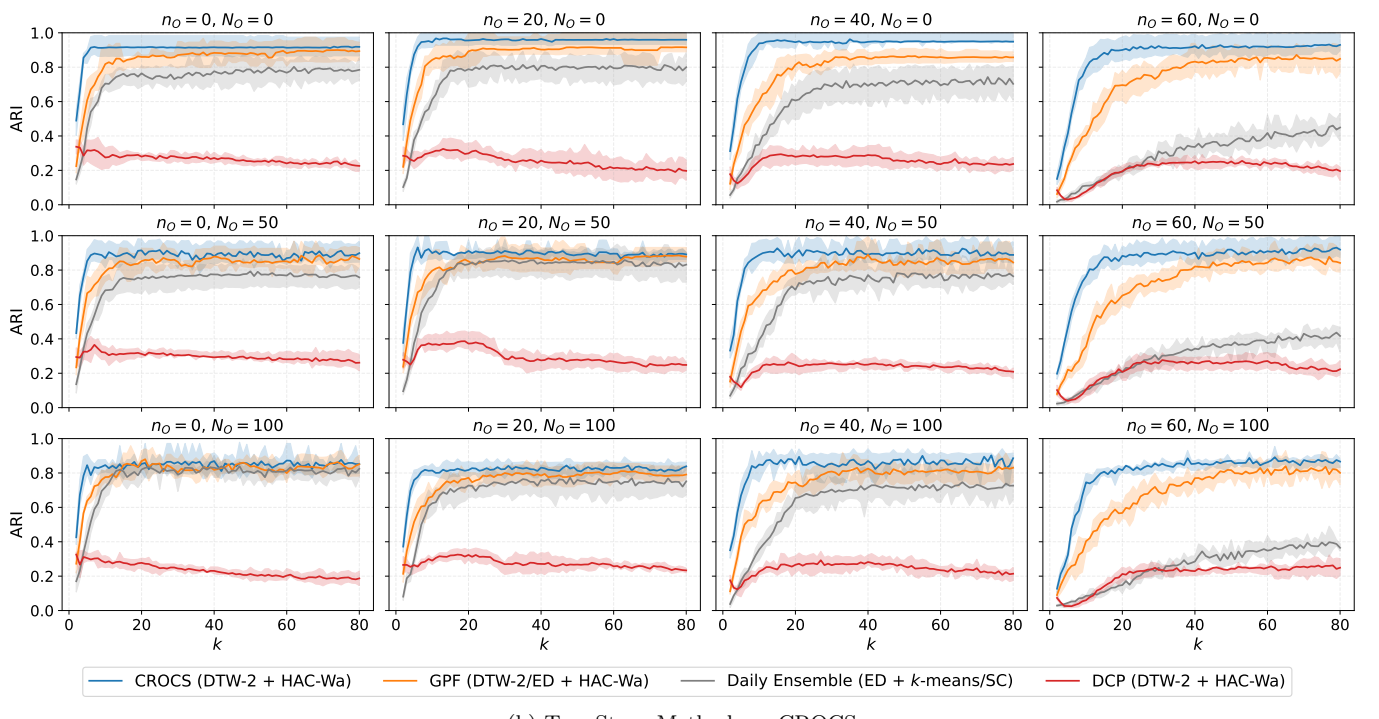


Figure 12: Mean ARI (with 50 percentile intervals) indicating recovery of synthetic consumer clusters by CROCS and other one and two-stage clustering methods proposed in the literature. Note that the results shown in (b) are for  $k^* = 8$ , though similar plots for the other values of  $k^*$  provided consistent results.

ods when identifying consumers with similar but asynchronously expressed consumption patterns, with the performance gap widening as real-world complexity increases.

## 5.5 Scalability

The practical value of a consumer clustering method depends not only on segmentation quality, but also on its ability to process datasets at real-world scales. To evaluate the computational performance of CROCS, we applied it to synthetic datasets comprising tens of thousands of consumers over a three-month (90 day) period. CROCS was implemented using DTW-2 with HAC-Wa and min-max normalisation. As discussed in Section 5.1, stage one runtime with HAC-Wa is consistently faster than with KMD and independent of the choice of  $k$ , while stage two runtime is similarly independent of the number of consumer clusters ( $K$ ).

Stage one clustering and the pairwise consumer distance matrix computation with WSMD were parallelised across 50 cores on a single node of a Linux HPC system equipped with AMD EPYC 7543 processors (2.8 GHz base clock). Jobs were executed in Python 3.12.3 with up to 256 GB memory (as required for the dataset size). Runtimes reported are wall-clock times for the first and second stages of clustering, inclusive of parallelisation overhead.

Recall that the computational complexity of CROCS is  $\mathcal{O}(mp^2 + k^2m^2)$ , where  $m$  is the number of consumers,  $p$  the number of days, and  $k$  the number of stage one clusters. Despite quadratic dependence on both  $m$  and  $p$ , in practice  $m \gg p$  is by far the more relevant case, as historical data more than a few years old is often of limited current segmentation value, while consumer populations can easily reach massive scales. Accordingly, we generated datasets with  $m \in \{5000, 10000, 20000, 40000, 80000\}$ . We also considered practical numbers of stage one clusters  $k \in \{2, 3, \dots, 30\}$  and numbers of consumer clusters  $K \in \{2, 3, \dots, 20\}$ .

Execution times for CROCS across the different parameter settings are reported in Figure 13. As expected, the quadratic dependence on  $m$  is evident: doubling the number of consumers consistently leads to about a fourfold increase in runtime, with a comparable effect observed when increasing  $k$  over the practical range considered. For reference, datasets of 10,000 consumers with  $k = 15$  completed in under two hours, while datasets of 80,000 consumers completed within two days. These datasets are far beyond the scales available in public datasets used in most prior smart meter clustering studies — typically under 7,000 consumers [110].

The results here show that CROCS maintains practical runtimes while preserving the flexibility needed to achieve meaningful and operationally useful clustering outcomes. Although our implementation was parallelised across 50 HPC cores, there remains scope for further optimisation, though future improvements may involve trade-offs between speed and segmentation quality, particularly for applications at even larger scales or when faster turnaround is required. Notably, we did not employ any of the available faster variants of clustering or distance computation — such as accelerated or approximate DTW variants [21], and parallel or approximate hierarchical clustering [30, 51] — suggesting that further efficiency gains are possible should such methods be incorporated. In addition, many practical applications could suitably be addressed by analysing representative samples rather than entire populations, making CROCS readily applicable at operationally relevant scales.

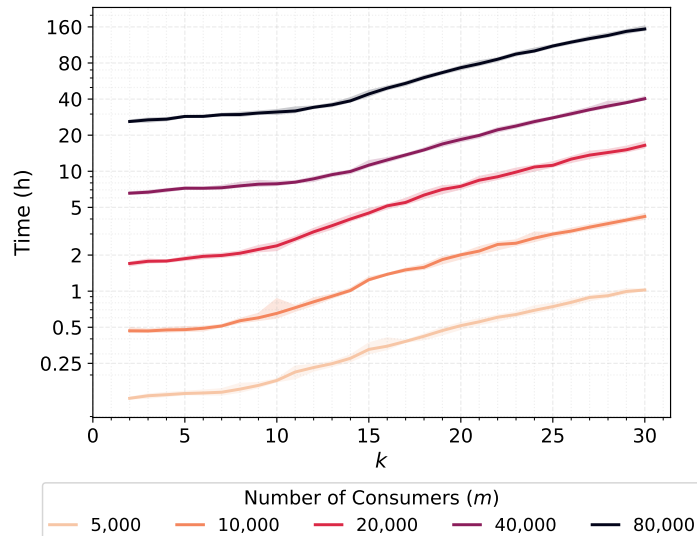


Figure 13: Execution time of CROCS (total wall-clock runtime in hours averaged over ten runs, inclusive of parallelisation overhead) when applied to datasets with varying numbers of consumers ( $m$ ) with  $p = 90$  DLPs per consumer. The data were clustered using DTW-2 with HAC-Wa and min-max normalisation, and results are shown on a log-scale for different numbers of stage one clusters ( $k$ ).

## 6 Real-World Application

We now demonstrate an application of the CROCS framework to the real-world AG dataset, examining consumer clusters across both Australian winter and summer periods. The winter period spanned from 1<sup>st</sup> June to 31<sup>st</sup> August 2012 inclusive, and summer from 1<sup>st</sup> December 2012 to 28<sup>th</sup> February 2013 inclusive. As discussed in Section 2.3, many energy retailers make a distinction between workdays and non-working<sup>8</sup> days due to the significance of coincident peak usage with commercial consumers. For this reason, only workdays within these windows were included in the analysis — leaving 65 and 60 days during the winter and summer periods respectively. By excluding non-working days, this application aligns with realistic use cases such as the design of weekday time-of-use tariffs or the targeting of other DR programs that aim to reduce significant weekday consumption peaks.

For this scenario, CROCS was implemented with min-max normalised DLPs, DTW-2, medoid prototypes and KMD for both clustering stages, though HAC-Wa was also considered. The number of stage one clusters ( $k$ ) and consumer clusters ( $K$ ) were varied, with selections guided by consideration of RVIs and the judgement of domain experts. In both cases,  $k = 15$  was found to sufficiently capture the range of consumers' DLP shapes, and  $K = 5$  provided a partition of the consumers into a practical number of distinct clusters for the hypothetical use cases.

Having introduced the concept of Refined RLSs in Section 3.3, we now compute them for the consumer clusters obtained in this application. The RRLSs provide hyperprototypes that summarise the common diurnal load patterns shared by consumers within each cluster, enhancing interpretability by making explicit the behavioural modes that define cluster membership.

As noted in Section 3.3, we do not prescribe any particular community detection method for identifying densely connected regions of the prototype graph. In this application, we employed the Leiden algorithm for its scalability and guarantee of well-connected communities [102]. In particular, the `leidenalg` Python package implementation was used with Reichardt–Bornholdt Erdős–Rényi (RBER) quality function [85], which incorporates vertex weights, and edge weights (obtained as the inverse of DTW-2 dissimilarities). Various quality functions are available in `leidenalg` which exploit different graph attributes — for instance, RBER and the Constant Potts Model (CPM) [101] make use of vertex weights and edge weights, while traditional modularity considers edge weights and directions. The use of vertex weights is particularly relevant in this application, as each node (prototype) already represents multiple DLPs, and the optimiser accounts for this when defining the size of communities in the quality function.

The RBER quality function was selected over both CPM and modularity for a few reasons. Like CPM, RBER includes a resolution parameter  $\gamma$  that enables the identification of both small and large communities, in contrast to modularity which struggles to resolve small but meaningful communities [101]. However, CPM imposes an absolute density cut-off, requiring all communities exceed the fixed threshold  $\gamma$  irrespective of the graph's overall structure. RBER instead defines community density relative to the global edge density  $\rho$ , requiring communities be denser than  $\gamma\rho$ . This relative formulation avoids the need to tune arbitrary absolute density thresholds for each prototype graph — a key advantage given that graph sizes can differ across consumer clusters. In any case, larger values of  $\gamma$  impose stricter density requirements, typically producing a greater number of smaller communities. Importantly, recognising minor communities of outlying prototypes separates them from the major communities, resulting in more meaningful coverage statistics.

Similar to the tuning of  $\gamma$  in [112], any desired number of communities was obtained by initialising  $\gamma$  at 0.02 and incrementing it in steps of 0.01 until the target number of communities was achieved. The hyperprototypes from a range of numbers of communities were evaluated by domain experts to ensure representativeness, striking a balance between concisely summarising typical daily load patterns and preserving operationally meaningful behavioural diversity present in each community.

The resulting summer and winter consumer partitions are presented in Figures 14 and 15 respectively, with each cluster's corresponding medoid and mean hyperprototypes shown in the two right hand panels. The left-hand panel shows the communities discovered in the respective prototype graphs, while the second panel from the left reports coverage statistics in terms of consumer coverage ( $x$ -axis) and day coverage ( $y$ -axis), both expressed as percentages. A relatively large number of hyperprototypes (10-40) were selected for each consumer cluster, many of which represent small communities with outlying consumption patterns not widely shared across the cluster. The major hyperprototypes that captured consumption patterns common to a large proportion of consumers are prominently represented with distinct colours in Figures 14 and 15, while outlying patterns are shown in a uniform navy blue tone.

The following sections examine the summer and winter partitions in detail, focusing on clusters' major hyperprototypes that capture the shared behavioural modes underlying weekday consumption.

### Summer Partition

All consumers in the AG Solar Home Electricity dataset possess some form of generation capacity, and variation in the extent of generation emerged as a key factor distinguishing clusters and patterns shared within clusters. Taken

<sup>8</sup>Incorporating both weekends and public holidays.

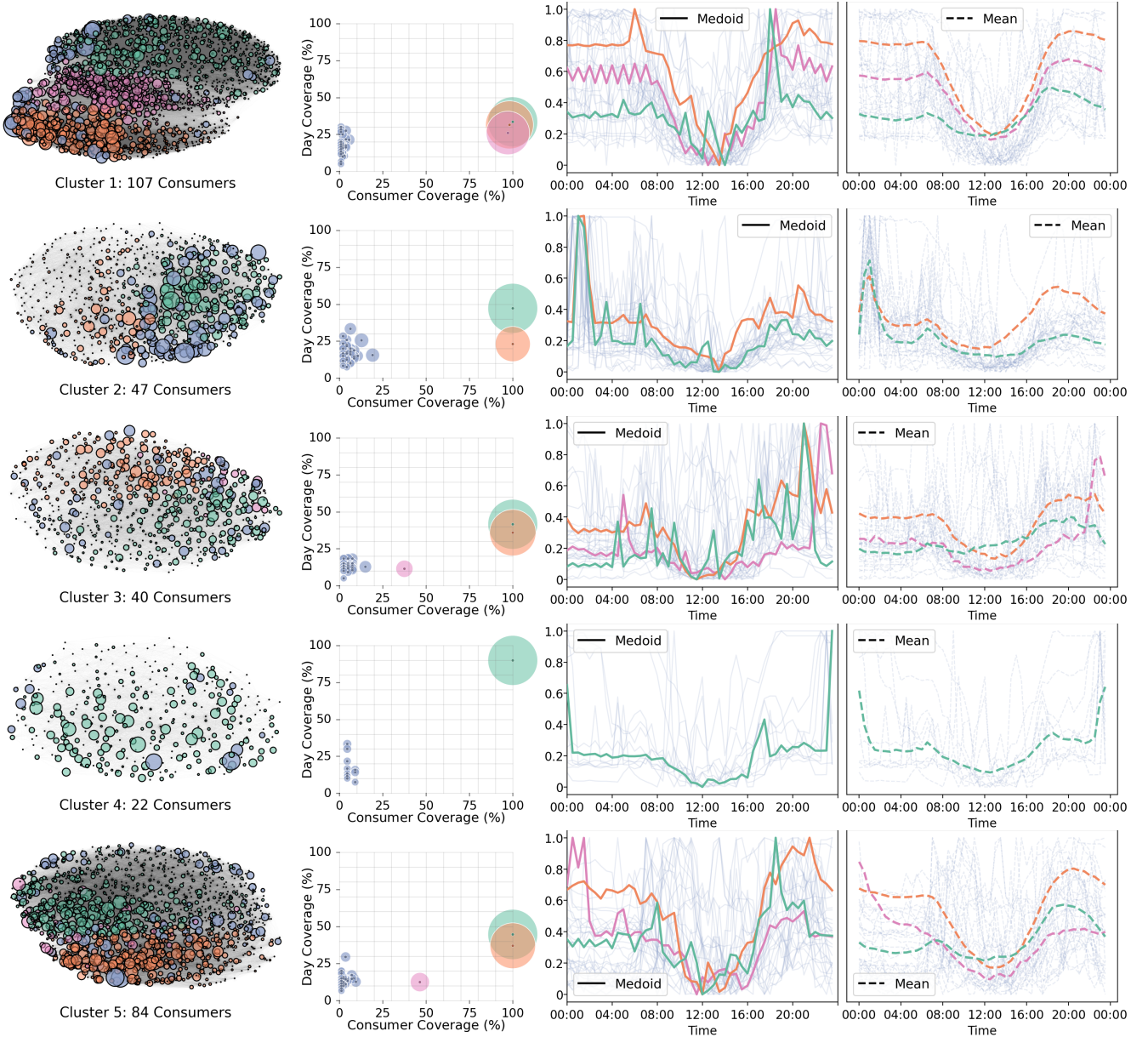


Figure 14: Five consumer clusters for a **summer** period from the Ausgrid dataset, showing the communities discovered in the prototype graphs on the left, coverage statistics plots, and hyperprototypes for each major community discovered (medoids and means) on the right. Workdays from 1st December 2012 to 28th February 2013 inclusive (60 days) were clustered using CROCS with min-max normalised DLPs, DTW-2,  $k = 15$ , medoid prototypes, and KMD for both stages. Major hyperprototypes representing common patterns shared by a significant proportion of consumers are highlighted with brightly coloured lines, while minor hyperprototypes capturing outlying consumption behaviours are shown in navy. Coverage statistics indicate the percentage of consumers ( $x$ -axis) and days ( $y$ -axis) represented by each hyperprototype, with circle sizes proportional to consumer coverage

together, consumers in Clusters 2, 3, and 4 showed relatively low levels of generation compared to their consumption, while those in Clusters 1 and 5 often exhibited generation comparable to or exceeding their demand.

Consumption patterns in cluster 1, the largest consumer group, were strongly differentiated by relative levels of generation. On approximately one third of days, households exhibited profiles dominated by significant generation, with only mild morning (06:00) and evening (20:00) peaks. Nonetheless, nearly all consumers displayed more substantial evening consumption around 18:00–19:00 on 60% of days with relatively moderate or mild levels of generation.

Cluster 2 was characterised by dominant post-midnight consumption peaks on about 75% of days, with minor morning (07:00) and evening (19:00–20:00) peaks. The outlying consumption prototypes also showed a tendency for peaks post midnight, with sporadic peak consumption elsewhere in the day.

Cluster 3 was characterised by minimal generation compared to consumption on 40% of days, and moderate generation on 35% of days. In either case, consumption peaked late in the evening between 20:00–21:00. For a small

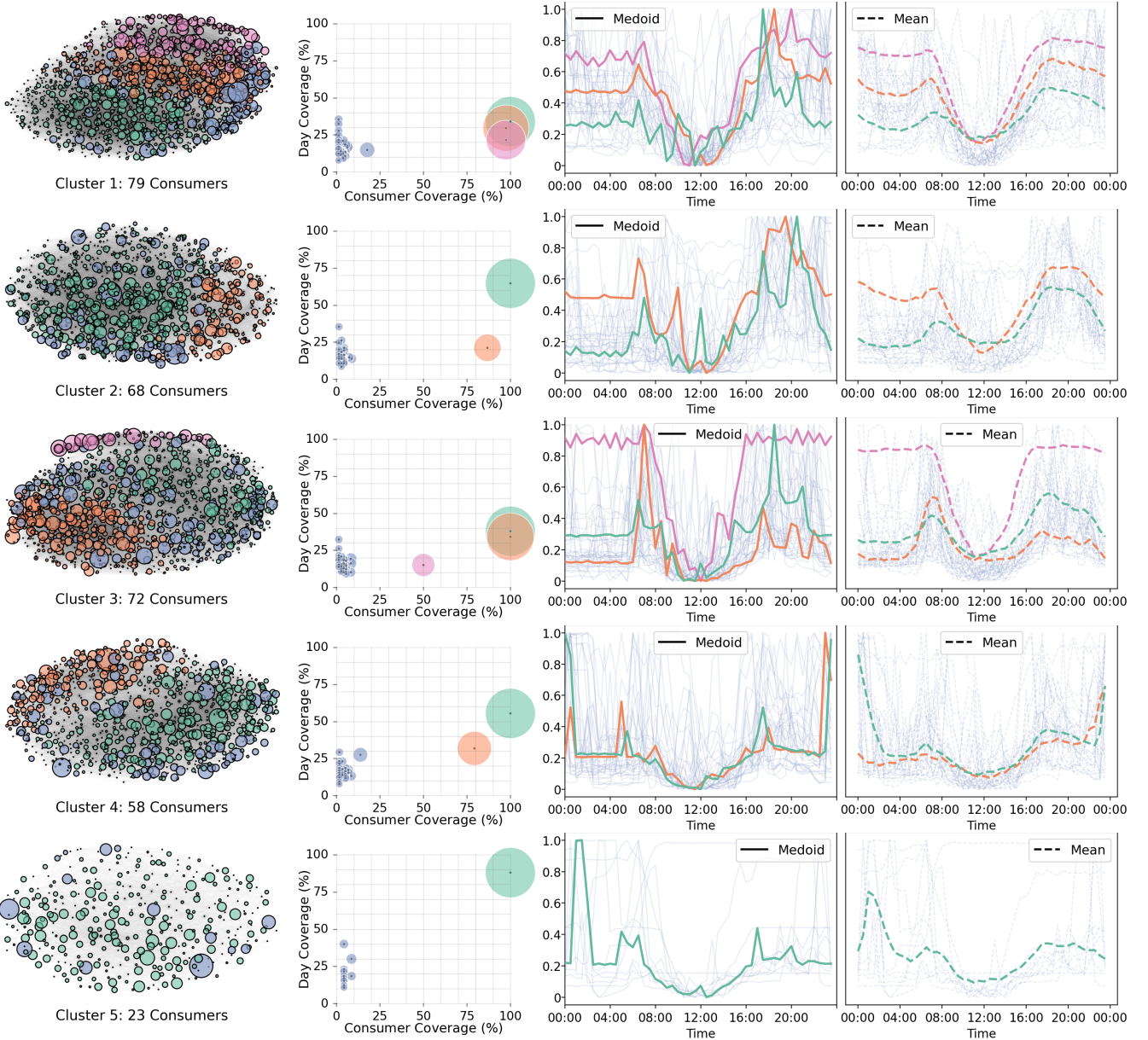


Figure 15: Five consumer clusters for a **winter** period from the Ausgrid dataset, showing the communities discovered in the prototype graphs on the left, coverage statistics plots, and hyperprototypes for each major community discovered (medoids and means) on the right. Workdays from 1st June to 31st August 2012 inclusive (65 days) were clustered using CROCS with min-max normalised DLPs, DTW-2,  $k = 15$ , medoid prototypes, and KMD for both stages. Major hyperprototypes representing common patterns shared by a significant proportion of consumers are highlighted with brightly coloured lines, while minor hyperprototypes capturing outlying consumption behaviours are shown in navy. Coverage statistics indicate the percentage of consumers ( $x$ -axis) and days ( $y$ -axis) represented by each hyperprototype, with circle sizes proportional to consumer coverage

subset of consumers, consumption peaked later again on 10% of days, just prior to midnight.

Cluster 4 was the smallest group and showed highly distinctive behaviour. For 90% of days, consumption was concentrated at or just after midnight. This could indicate occupants with late-night routines such as shift workers, or could indicate the presence of appliances such as electric hot water systems, pool pumps. Minor peaks around 07:00 and 19:00 were also consistently observed for these consumers, as evidenced by the green mean hyperprototype.

Cluster 5's green hyperprototype, accounting for all consumers on 45% of days, had a very similar shape to cluster 1's green hyperprototype, with an evening consumption peak around 19:00 and relatively moderate generation. However on another 35% of days, a less prominent and more sustained peak in consumption could be observed later in the evening, around 20:00. Additionally, around 45% of consumers used minimal electricity throughout the day after an early morning peak on 15% of days.

## Winter Partition

The consumer partition was more balanced for the winter period compared to summer, suggesting that consumers demonstrate greater uniformity through warmer seasons. This supports our earlier findings in relation to Figure 7 which showed that more diverse consumption patterns tend to be seen during cooler seasons.

Similar to its summer counterpart, Cluster 1's hyperprototypes were strongly differentiated by relative levels of generation. All three major hyperprototypes (accounting for about 85% of days) from cluster 1 exhibit moderate morning consumption peaks around 07:00 with varying degrees of evening consumption typically centred between 17:30–18:30. Generation was significant compared to consumption on just over half of the days from this period (pink and orange hyperprototypes).

Cluster 2 consumers, by contrast, exhibited limited generation relative to consumption on around two thirds of days, and significant consumption peaks throughout the evening between 17:00–21:00. Around 20% of days displayed higher generation for around 85% of consumers, coinciding with a slight shift in evening usage later and morning usage earlier — suggesting a degree of responsiveness to weather signals.

Consumption peaked in the morning around 07:00–08:00 for the consumers in cluster 3 on 35% of days, and in the evening around 18:00–19:00 on another 40% of days. For around 50% of consumers in this cluster, a “standby” profile — with significant generation and almost negligible consumption — was exhibited on 15% of days.

Cluster 4 resembled the summer counterpart, but with increased membership. Just over half of days were dominated by midnight peaks, with a tendency for slightly pre-midnight peaks for around 80% of consumers on another one third of days. Secondary morning (05:00–07:00) and early evening (17:00–18:00) peaks were also present, though less pronounced.

Cluster 5, the smallest winter group, was similar to the summer Cluster 2 but reduced in size. For 90% of days, households showed strong peaks in the early morning, supplemented by minor morning (06:00–07:00) and evening (17:00–19:00) peaks.

## Implications

The coverage plots in Figures 14 and 15 reveal that, within clusters, some consumers are not represented as well as the majority by the main hyperprototypes. For example, in winter cluster 5 one consumer had about 40% of their days not captured by the dominant hyperprototype, whereas most others were covered to a much greater extent. Similar patterns can be observed across the other summer and winter clusters. In practice, program designers may wish to acknowledge this variability and prioritise targeting consumers whose behaviours are most closely aligned with the dominant hyperprototypes, or with their cluster's RRLS more broadly. A natural way to assess this is by computing WSMD distances between each consumer's RLS and their cluster's RRLS, weighting hyperprototypes by prevalence. Such an approach identifies consumers who are most representative of the cluster's shared behavioural modes, and hence most likely to respond in a predictable way to interventions. Alternatively, filtering could emphasise high-consumption households to maximise aggregate impact, while excluding those below a minimum consumption threshold reduces the risk of limited returns.

Meanwhile, many clusters did display clear and recurrent consumption patterns that cover the majority of consumers, and these provide a strong foundation for the design and targeting of DSM and DR strategies. Beyond these initial phases, CROCS also provides a practical means to evaluate program outcomes. Rather than re-clustering the entire dataset, utilities could revisit the consumers within a given cluster after some period of time, recomputing their stage one behaviours and pairwise similarities to derive updated hyperprototypes. Shifts in the prevalence or shape of these hyperprototypes would then indicate whether an intervention, such as a time-of-use tariff, appears to have had the intended effect. In this way, CROCS supports not only the design but also the ongoing assessment and refinement of demand-side strategies.

## 7 Discussion

In Section 2.3 we identified a series of eight methodological challenges that constrain the effectiveness of existing consumer clustering methodologies. The following discussion considers each of these limitations in turn and examines how CROCS addresses them, drawing on both the framework's design and the experimental evidence from Section 5. We also highlight directions for further research.

### (i) Capturing Intra-Consumer Variation

A core strength of CROCS lies in its ability to preserve behavioural diversity when representing individual consumers for clustering. The Representative Load Set central to the CROCS framework provides a flexible, consumer-specific summary, capturing both the shape of diurnal patterns and the frequency with which they occur in an unsupervised manner. As demonstrated in Section 5.2, the local RLS efficiently achieves lower reconstruction error than other

load-profile based representations that either use single profiles (e.g., RLP, DCP), or multiple profiles discovered globally (e.g., GPF). Importantly, this performance remains robust even when the number of stage one clusters ( $k$ ) is overestimated. As demonstrated in Section 5.1, CROCS does not require fine-tuned parameter selection to yield meaningful results. This is because the WSMD distance acknowledges prototype similarity *and* weights according to prevalence, so verbose behavioural summaries with large  $k$  still lead to effective consumer clusterings.

Finally, by retaining both variation and individuality, the RLS also supports downstream applications that require analysis at the level of individual consumers. For example, such analysis may be required for: identifying consumers with anomalous changes to their consumption patterns due to occupancy changes, uptake of electric vehicles or household batteries, other appliance changes, or energy fraud; identifying consumers demonstrating a rebound effect (peak shifting) in response to TOU tariff structures [114]; or monitoring the success of demand-side interventions and other behavioural transitions over time.

#### (ii) Preserving Common Intra-Consumer Variation in Clusters

Given the emphasis in the literature on the importance of capturing intra-consumer variation, it would be incomplete to then discard that variation when it unites consumers within clusters. The RRLS concept within the CROCS framework instead preserves that shared variation, allowing distinct but prevalent modes of behaviour to be retained rather than merged into single profiles.

As demonstrated in Section 6, many real-world consumer clusters were characterised by a small number of distinct behavioural modes that were shared across the majority of members. Representing each of these modes with their own profile makes explicit the concrete behaviours that connect consumers within a group, enhancing interpretability and providing a firm basis for downstream applications.

#### (iii) Recognition of Asynchronous Consumer Similarity

Because the RLS representation is not temporally anchored, CROCS can cluster together consumers that exhibit similar diurnal patterns whether they occur on the same, or on different days. As illustrated between Figures 9 and 10, such asynchronous pairs are likely far more numerous than synchronous pairs that display similar diurnal patterns which consistently align on the same days. While some other methods are in principle capable of recognising similar yet asynchronous pairs of consumers, it was demonstrated in Section 5.4 that CROCS consistently does so more effectively across a range of dataset conditions.

It bears emphasising that CROCS extends recognition to asynchronous similarity while fully retaining its capacity to detect synchronous similarity. This capability is significant for downstream applications where concurrency isn't strictly essential — for instance, in selecting households for distributed energy resource adoption or curtailable service incentives, or designing and deploying TOU tariffs. It also supports equity in program design, by ensuring that consumers with similar behavioural potential are not excluded from DSM or DR opportunities simply because their schedules are atypical.

#### (iv) Robustness to Behavioural Anomalies

The WSMD distance measure used in the CROCS framework weights consumption patterns according to their frequency when assessing consumer similarity. In this way, unusual behaviours are acknowledged within consumer RLSs but prevented from distorting the clustering outcome. Experiments in Section 5.3 demonstrate that WSMD consistently outperforms alternative set-to-set distances — even in the presence of significant numbers of outlying diurnal patterns. Unlike other distances such as SMD or MHD, it also required the smallest overestimation of  $k$  to achieve reliable results, making it well suited to real-world data where the prevalence of outliers is unknown. This robustness provides greater stability in consumer segmentation while still acknowledging anomalous behaviour in a way that facilitates further inspection.

#### (v)-(vii) Flexible Handling of Non-Synchronised Data, Regular Discontinuities, and Missing Data

CROCS flexibly handles irregularities in input data that commonly hinder other consumer clustering approaches, owing primarily to the RLS consumer representation.

Because the RLS is computed independently on each consumer's available set of DLPs, the framework does not require time-synchronised or equal-length series. Consumers with staggered installation dates or different quantities of relevant historical data can therefore be included without truncating longer records or discarding more recent installations.

The method is likewise robust to regular discontinuities, such as those created when analysing workdays separately from weekends (as in Section 6). In CROCS, gaps between selected subsets of days do not create spurious temporal dependencies in the RLS representation, unlike approaches that require concatenating subsequences of long time series.

Finally, CROCS can accommodate sizeable quantities of missing data simply by omitting affected days from the RLS computation, avoiding the need for large-scale imputation or consumer exclusion. This ensures that segmentation makes use of the maximum amount of reliable information while maintaining representativeness across the population.

By remaining inclusive of consumers with incomplete, non-synchronised, or discontinuous data, CROCS ensures valuable data are not wasted, and provides more equitable foundations for DSM and DR program design.

### (viii) Scalability and Practical Deployment

While scalability is essential for practical deployment, computational efficiency should not come at the cost of segmentation quality. CROCS maintains this balance by decomposing the problem into two stages: the first stage of clustering for local consumer representations is fully independent and parallelisable, while computation of WSMD distances between compact consumer RLSs can also be parallelised in the second stage. This contrasts with effective global approaches such as GPF, which scale poorly with the number of consumers and whose representations must be entirely recomputed whenever new consumers are added. As shown in Section 5.5, CROCS scales quadratically with the number of consumers while still achieving runtimes that render large-scale consumer segmentation practically feasible, in contrast to the much smaller populations typically addressed in prior studies. In addition, robustness to overestimation of the stage one parameter  $k$  reduces the need for costly parameter tuning, providing a practical configuration strategy at scale.

## 7.1 Future Directions

CROCS addresses key shortcomings of existing methods, yet there are opportunities for further refinement and extension to maximise its utility in practical DSM and DR contexts.

Firstly, the community detection algorithm used to determine the RRLS summaries for consumer clusters, while effective for identifying shared behaviours, currently scales less efficiently than the two primary stages of CROCS that identify consumer segments. Future work could assess the trade-off between representation quality and scalability in more lightweight alternative algorithms that utilise simpler graph constructions obtained by omitting edge directions, node weights or edge weights (or combinations thereof). Moreover, it could also be productive to consider alternative transformations of the WSMD dissimilarities into connection strengths (e.g. by subtracting dissimilarities from an appropriate maximum) or the use of community detection algorithms that operate directly on dissimilarities as edge weights instead. A more radical option would be to replace the graph conception entirely with a direct time series clustering of the prototypical DLPs.

Secondly, while the popular min–max normalisation was adopted in this study to ensure that clustering emphasised shape rather than magnitude, a range of alternatives have been used throughout the literature — yet there is little systematic understanding of when and why one should be preferred. Future research could therefore evaluate the suitability of different procedures within the CROCS framework, and develop recommendations for which procedures are most appropriate for particular applications. For instance, alternative schemes such as  $z$ -normalisation or unit-norm scaling [116] may provide distinct advantages. Some form of selective normalisation could also prove beneficial — for instance, clustering unnormalised DLPs (or DLPs extracted from normalised long time series) in the first stage, which could differentiate shapes associated with higher and lower consumption levels for individual consumers — with normalisation applied only to prototypes in the second stage to enable comparisons between consumers. Relatedly, pre-binning consumers by overall consumption level and then performing clustering separately on consumers within each bin, as suggested by [99, 100], could provide an effective pathway for scaling segmentation to many hundreds of thousands or even millions of consumers.

Thirdly, CROCS could be extended beyond segmentation by hybridising it with forecasting tasks. Stage one prototypes within consumers’ RLSs provide natural primitives for next-day prediction, while stage two clusters could be utilised for aggregate-level forecasting. Sequence-based forecasting approaches such as Pattern Sequence Forecasting [63, 62] or Markov-based forecasting [97] could be applied to consumers’ stage one cluster labels, providing additional utility from the computational effort invested in stage one clustering. Future research could compare the accuracy of such CROCS-informed forecasting with existing methods. In some applications, segmentation and forecasting may even serve as complementary goals, with this line of inquiry offering a pathway to integrate both within a single framework for operational use.

Finally, while CROCS has been developed and explored in this paper in the context of smart-meter data, the framework is certainly applicable to a broader class of problems where synchronised *and* asynchronous similarities across sub-periods are of interest. For instance, household water consumption is highly analogous, where daily profiles of water use could be clustered in stage one, with stage two then grouping households by the distribution of these patterns. Electric vehicle charging time series provides another example, where individual charging sessions provide an analogue of the stage one “sub-periods” to be characterised with typical charging curves, while stage two would group drivers or charging sites according to the mix of sessions they exhibit, likely supporting infrastructure planning, and grid integration. Beyond time series, CROCS could also be applied to domains with repeated feature-

described events across multiple entities, such as sports analytics or retail. In these cases, stage one would cluster event-level feature vectors and stage two would group entities (players or teams, customers or users) according to their prototypical features discovered in stage one. These examples are far from exhaustive, but they illustrate the broader potential of CROCS to uncover interpretable behavioural structures across a wide variety of dataset formats and domains.

## 8 Conclusion

This study has introduced CROCS — Clustered Representations Optimising Consumer Segmentation — a novel two-stage clustering framework designed to address the eight methodological challenges we identified in our review of existing approaches. In the first stage, each consumer’s daily load profiles are clustered independently to produce a high-quality, local consumer representation via cluster prototypes. The resulting Representative Load Sets (RLSs) provide rich yet compact summaries of each consumer’s typical consumption patterns, preserving intra-consumer variation in an interpretable form, while naturally accommodating non-synchronised data, regular discontinuities, and missing data. In the second stage, consumers are clustered by comparing their RLSs using the Weighted Sum of Minimum Distances (WSMD). This set-to-set distance incorporates all prototypical behaviours while weighting them by prevalence, enabling the discovery of both synchronous and asynchronous similarity between consumers and reducing the influence of anomalous patterns. Finally, we developed an optional cluster-level representation, the Refined RLS (RRLS). Constructed directly from the similarity structure revealed by CROCS, RRLSs summarise consumer clusters with multiple hyperprototypes that represent the distinct behavioural modes shared across members. This avoids the loss of nuance that occurs when clusters are compressed into a single profile, thereby providing a more interpretable and faithful characterisation of consumer groups discovered by CROCS.

Our experimental analyses revealed an important and under-explored property of electricity consumption data: consumers often express similar diurnal behaviours asynchronously — exhibiting highly similar patterns but on different calendar days. We showed that pairs of such consumers appear more common than those where similar behaviours are temporally aligned, highlighting the limitations of clustering methods that rely on calendar synchronisation. CROCS also proved the most effective at detecting such asynchronous similarity, outperforming a broad range of existing methodologies — including those that in principle should also recognise asynchronous similarity. This finding has important implications for DSM and DR program design, as it demonstrates that many consumers with similar potential or suitability may be misclassified when relying on temporally anchored approaches.

Beyond this key result, our experiments validated the framework’s design choices while establishing clear guidance for its application. Most notably, simple overestimation of the stage one parameter  $k$  — the number of prototypes in each consumer’s RLS — proved to be a robust and practical configuration strategy for the framework’s sole parameter. The RLS also consistently outperformed alternative single- and multi-*profile* representations, achieving lower reconstruction error across a wide range of practical  $k$ . WSMD emerged as the most effective set-to-set distance, demonstrating robustness to outliers and working particularly well in combination with the overestimation strategy. Furthermore, CROCS demonstrated practical feasibility through a structure that is readily parallelisable and open to further optimisation. In our application to Australian smart meter data, hyperprototypes and their coverage statistics yielded interpretable seasonal summaries, clarifying the concrete daily consumption patterns that brought consumers together within the same cluster.

Beyond consumer segmentation, CROCS can also provide insights at the level of individual consumers, with stage one clustering supporting tasks such as anomaly detection, monitoring behavioural change, and identifying the uptake of new technologies. The framework is also inherently modular; while we implemented it using min–max normalisation with constrained Dynamic Time Warping and either  $k$ -medoids or Ward’s hierarchical clustering for consistency with comparative studies [115], CROCS can readily adopt alternative methodologies as required. By unifying methodological rigour with practical scalability, CROCS marks a step forward in behaviour-centric consumer segmentation — offering a robust and extensible framework that enhances the analytical value of smart meter data while strengthening the operational foundations of DSM and DR strategies in increasingly complex electricity systems.

## References

- [1] Milad Afzalan, Farrokh Jazizadeh, and Hoda Eldardiry. Two-Stage Clustering of Household Electricity Load Shapes for Improved Temporal Pattern Representation. *IEEE Access*, 9:151667–151680, 2021.
- [2] Charu C. Aggarwal, Alexander Hinneburg, and Daniel A. Keim. On the surprising behavior of distance metrics in high dimensional space. *Lecture Notes in Computer Science (including subseries Lecture Notes in Artificial Intelligence and Lecture Notes in Bioinformatics)*, 1973:420–434, 2001.
- [3] Charu C. Aggarwal and Chandan K. Reddy. *Data Clustering: Algorithms and Applications*. Chapman and Hall/CRC, New York, 1st edition, 2014.

[4] Saeed Aghabozorgi, Ali Seyed, and Teh Ying Wah. Time-series clustering – A decade review. *Information Systems*, 53:16–38, 2015.

[5] Rajesh K. Ahir and Basab Chakraborty. A novel cluster-specific analysis framework for demand-side management and net metering using smart meter data. *Sustainable Energy, Grids and Networks*, 31:100771, 2022.

[6] Nameer Al Khafaf, Mahdi Jalili, and Peter Sokolowski. A Novel Clustering Index to Find Optimal Clusters Size with Application to Segmentation of Energy Consumers. *IEEE Transactions on Industrial Informatics*, 17(1), 2021.

[7] Andres M. Alonso, Eduardo Martin, Alicia Mateo, Francisco J. Nogales, Carlos Ruiz, and Andrea Veiga. Clustering Electricity Consumers: Challenges and Applications for Operating Smart Grids. *IEEE Power and Energy Magazine*, 20(3):54–63, 2022.

[8] Andres M. Alonso, Francisco J. Nogales, and Carlos Ruiz. Hierarchical Clustering for Smart Meter Electricity Loads Based on Quantile Autocovariances. *IEEE Transactions on Smart Grid*, 11(5), 2020.

[9] Ioannis Antonopoulos, Valentin Robu, Benoit Couraud, Desen Kirli, Sonam Norbu, Aristides Kiprakis, David Flynn, Sergio Elizondo-Gonzalez, and Steve Wattam. Artificial intelligence and machine learning approaches to energy demand-side response: A systematic review. *Renewable and Sustainable Energy Reviews*, 130(June):109899, 2020.

[10] David Arthur and Sergei Vassilvitskii. k-means++: The Advantages of Careful Seeding. Technical Report 2006-13, Stanford InfoLab, 6 2006.

[11] Benjamin Auder, Jairo Cugliari, Yannig Goude, and Jean Michel Poggi. Scalable clustering of individual electrical curves for profiling and bottom-up forecasting. *Energies*, 11(7):1–22, 2018.

[12] Ausgrid. Solar home electricity data, 2013.

[13] Ausgrid. Smart-Grid Smart-City Customer Trial Data, 2014.

[14] Australian Bureau of Statistics. Energy Account, Australia, 2023.

[15] Australian Bureau of Statistics. Working arrangements. Technical Report 6336.0, Australian Bureau of Statistics, 2024.

[16] Australian Energy Market Commission. Accelerating Smart Meter Deployment, Rule determination. Technical report, AEMC, Sydney, 11 2024.

[17] Australian Energy Market Operator. Power System Requirements. Technical report, AEMO, 2020.

[18] Santiago Bañales, Raquel Dormido, and Natividad Duro. Smart Meters Time Series Clustering for Demand Response Applications in the Context of High Penetration of Renewable Energy Resources. *Energies 2021, Vol. 14, Page 3458*, 14(12):3458, 6 2021.

[19] Fatima Batool and Christian Hennig. Clustering with the Average Silhouette Width. *Computational Statistics and Data Analysis*, 158:107190, 2021.

[20] Sue Bedingfield, Damminda Alahakoon, Hiran Genegedera, and Naveen Chilamkurti. Multi-granular electricity consumer load profiling for smart homes using a scalable big data algorithm. *Sustainable Cities and Society*, 40(August 2017):611–624, 2018.

[21] Nurjahan Begum, Liudmila Ulanova, Jun Wang, and Eamonn Keogh. Accelerating Dynamic Time Warping Clustering with a Novel Admissible Pruning Strategy. In *Proceedings of the 21th ACM SIGKDD International Conference on Knowledge Discovery and Data Mining*, KDD '15, page 49–58, New York, NY, USA, 2015. Association for Computing Machinery.

[22] T. Bobmann and I. Staffell. The shape of future electricity demand: Exploring load curves in 2050s Germany and Britain. *Energy*, 90:1317–1333, 2015.

[23] Vichalia Zapata Castillo, Harmen Sytze de Boer, Raúl Maícas Muñoz, David E.H.J. Gernaat, René Benders, and Detlef van Vuuren. Future global electricity demand load curves. *Energy*, 258(July), 2022.

[24] Tao Chen, Kun Qian, Antti Mutanen, Bjorn Schuller, Pertti Jarventausta, and Wencong Su. Classification of electricity customer groups towards individualized price scheme design. In *2017 North American Power Symposium, NAPS 2017*, number 1, pages 2–5, 2017.

[25] Gianfranco Chicco. Overview and performance assessment of the clustering methods for electrical load pattern grouping. *Energy*, 42(1):68–80, 2012.

[26] Gianfranco Chicco, Roberto Napoli, and Federico Piglione. Comparisons Among Clustering Techniques for Electricity Customer Classification. *IEEE Transactions on Power Systems*, 21(2):933–940, 2006.

[27] Gianfranco Chicco, Roberto Napoli, Petru Postolache, Mircea Scutariu, and Cornel Toader. Electric energy customer characterisation for developing dedicated market strategies. *2001 IEEE Porto Power Tech Proceedings*, 1:371–377, 2001.

[28] Gianfranco Chicco, Roberto Napoli, Petru Postolache, Mircea Scutariu, and Cornel Toader. Customer characterization options for improving the tariff offer. *IEEE Transactions on Power Systems*, 18(1):381–387, 2003.

[29] Jacob Cohen. A Coefficient of Agreement for Nominal Scales. *Educational and Psychological Measurement*, 20(1):37–46, 1960.

[30] Manoranjan Dash, Simona Petrucci, and Peter Scheuermann. Efficient Parallel Hierarchical Clustering. In Marco Danelutto, Marco Vanneschi, and Domenico Laforenza, editors, *Euro-Par 2004 Parallel Processing*, pages 363–371, Berlin, Heidelberg, 2004. Springer Berlin Heidelberg.

[31] Sima Davarzani, Ioana Pisica, and Gareth A. Taylor. Study of missing meter data impact on domestic load profiles clustering and characterization. *Proceedings - 2016 51st International Universities Power Engineering Conference, UPEC 2016*, 2017-Janua:1–6, 2016.

[32] Matheus Alberto de Souza, José L.R. Pereira, Guilherme de O. Alves, Bráulio C. de Oliveira, Igor D. Melo, and Paulo A.N. Garcia. Detection and identification of energy theft in advanced metering infrastructures. *Electric Power Systems Research*, 182(December 2019):106258, 2020.

[33] Ian Dent, Tony Craig, Uwe Aickelin, and Tom Rodden. Variability of behaviour in electricity load profile clustering: Who does things at the same time each day? *Lecture Notes in Computer Science (including subseries Lecture Notes in Artificial Intelligence and Lecture Notes in Bioinformatics)*, 8557 LNAI:70–84, 2014.

[34] Thomas Eiter and Heikki Mannila. Distance measures for point sets and their computation. *Acta Informatica*, 34:109–133, 1997.

[35] Eurostat. Energy statistics - an overview, 2024.

[36] Giuseppe Fenza, Mariacristina Gallo, and Vincenzo Loia. Drift-aware methodology for anomaly detection in smart grid. *IEEE Access*, 7:9645–9657, 2019.

[37] Christoph Flath, David Nicolay, Tobias Conte, Clemens Van Dinther, and Lilia Filipova-Neumann. Cluster analysis of smart metering data: An implementation in practice. *Business and Information Systems Engineering*, 4(1):31–39, 2012.

[38] Santo Fortunato. Community detection in graphs. *Physics Reports*, 486(3-5):75–174, 2010.

[39] Santo Fortunato and Darko Hric. Community detection in networks : A user guide. *Physics Reports*, 659:1–44, 2016.

[40] Guojun Gan, Chaoqun Ma, and Jianhong Wu. *Data clustering : theory, algorithms, and applications*. Society for Industrial and Applied Mathematics, Philadelphia, 2nd edition, 10 2007.

[41] G. R. Hemanth and S. Charles Raja. Proposing suitable data imputation methods by adopting a Stage wise approach for various classes of smart meters missing data – Practical approach. *Expert Systems with Applications*, 187(May 2021):115911, 2022.

[42] Christopher Holder, Matthew Middlehurst, and Anthony Bagnall. A review and evaluation of elastic distance functions for time series clustering. *Knowledge and Information Systems*, pages 1–45, 9 2023.

[43] Lawrence Hubert and Phipps Arabie. Comparing partitions. *Journal of Classification*, 2(1):193–218, 1985.

[44] Ali Javed, Byung Suk Lee, and Donna M. Rizzo. A benchmark study on time series clustering. *Machine Learning with Applications*, 1(September):100001, 2020.

[45] L Jin, Lee D, A Sim, S Borgeson, K Wu, C. A. Spurlock, and A Todd. Comparison of Clustering Techniques for Residential Energy Behavior using Smart Meter Data. In *The AAAI-17 Workshop on Artificial Intelligence for Smart Grids and Smart Buildings*, pages 260–266, 2017.

[46] Ramanpreet Kaur and Dušan Gabrijelčič. Behavior segmentation of electricity consumption patterns: A cluster analytical approach. *Knowledge-Based Systems*, 251, 9 2022.

[47] Eamonn Keogh and Shruti Kasetty. On the need for time series data mining benchmarks: A survey and empirical demonstration. *Proceedings of the ACM SIGKDD International Conference on Knowledge Discovery and Data Mining*, pages 102–111, 2002.

[48] Y. Kiguchi, M. Weeks, and R. Arakawa. Predicting winners and losers under time-of-use tariffs using smart meter data. *Energy*, 236:121438, 2021.

[49] Hyojeoung Kim, Sujin Park, and Sahm Kim. Time-series clustering and forecasting household electricity demand using smart meter data. *Energy Reports*, 9, 2023.

[50] Arthur Lin Ku, Yueming (Lucy) Qiu, Jiehong Lou, Destenie Nock, and Bo Xing. Changes in hourly electricity consumption under COVID mandates: A glance to future hourly residential power consumption pattern with remote work in Arizona. *Applied Energy*, 310(September 2021):118539, 2022.

[51] Meelis Kull and Jaak Vilo. Fast approximate hierarchical clustering using similarity heuristics. *BioData Mining*, 1(1):9, 2008.

[52] Sammukh R. Kuppannagari, Yao Fu, Chung Ming Chueng, and Viktor K. Prasanna. Spatio-Temporal Missing Data Imputation for Smart Power Grids. In *e-Energy 2021 - Proceedings of the 2021 12th ACM International Conference on Future Energy Systems*, pages 458–465, 2021.

[53] Jungsuk Kwac, June Flora, and Ram Rajagopal. Household energy consumption segmentation using hourly data. *IEEE Transactions on Smart Grid*, 5(1):420–430, 2014.

[54] Cheng Ping Lai, Pau Choo Chung, and Vincent S. Tseng. A novel two-level clustering method for time series data analysis. *Expert Systems with Applications*, 37(9):6319–6326, 2010.

[55] Eunjung Lee, Jinho Kim, and Dongsik Jang. Load profile segmentation for effective residential demand response program: Method and evidence from Korean pilot study. *Energies*, 16(3), 3 2020.

[56] Ran Li, Furong Li, Senior Member, and Nathan D Smith. Multi-Resolution Load Profile Clustering for Smart Metering Data. *IEEE Transactions on Power Systems*, 31(6):4473–4482, 2016.

[57] Xuefang Li, Qiang Zhang, Zhanglin Peng, Anning Wang, and Wanying Wang. A data-driven two-level clustering model for driving pattern analysis of electric vehicles and a case study. *Journal of Cleaner Production*, 206:827–837, 1 2019.

[58] Yuancheng Li, Panpan Guo, and Xiang Li. Short-Term Load Forecasting Based on the Analysis of User Electricity Behavior. *Algorithms*, 9(4), 2016.

[59] J Lin. Divergence measures based on the Shannon entropy. *IEEE Transactions on Information Theory*, 37(1):145–151, 1991.

[60] Jessica Lin, Eamonn Keogh, Li Wei, and Stefano Lonardi. Experiencing SAX: a novel symbolic representation of time series. *Data Mining and Knowledge Discovery 2007* 15:2, 15(2):107–144, 4 2007.

[61] Michele R.B. Malinowski and Richard J. Povinelli. Using Smart Meters to Learn Water Customer Behavior. *IEEE Transactions on Engineering Management*, 69(3):729–741, 2022.

[62] Francisco Martínez-Álvarez, Alicia Troncoso, José C. Riquelme, and Jesús S. Aguilar-Ruiz. LBF: A labeled-based forecasting algorithm and its application to electricity price time series. In *Proceedings - IEEE International Conference on Data Mining, ICDM*, number 453, pages 453–461, 2008.

[63] Francisco Martínez-Álvarez, Alicia Troncoso, José C. Riquelme, and Jesús S. Aguilar Ruiz. Energy time series forecasting based on pattern sequence similarity. *IEEE Transactions on Knowledge and Data Engineering*, 23(8):1230–1243, 2011.

[64] Fintan McLoughlin, Aidan Duffy, and Michael Conlon. A clustering approach to domestic electricity load profile characterisation using smart metering data. *Applied Energy*, 141:190–199, 2015.

[65] M. L. Menendez, J. A. Pardo, and L. Pardo. Csiszar's phi-divergences for testing the order in a Markov chain. *Statistical Papers*, 42:313–328, 2001.

[66] Fanlin Meng, Qian Ma, Zixu Liu, and Xiao Jun Zeng. Multiple dynamic pricing for demand response with adaptive clustering-based customer segmentation in smart grids. *Applied Energy*, 333, 3 2023.

[67] Kevin Mets, Frederick Depuydt, and Chris Develder. Two-Stage Load Pattern Clustering Using Fast Wavelet Transformation. *IEEE Transactions on Smart Grid*, 7(5):2250–2259, 9 2016.

[68] Vasilis Michalakopoulos, Elissaios Sarmas, Ioannis Papias, Panagiotis Skaloumpakas, Vangelis Marinakis, and Haris Doukas. A machine learning-based framework for clustering residential electricity load profiles to enhance demand response programs. *Applied Energy*, 361, 5 2024.

[69] Glenn W Milligan. Clustering Validation: Results and Implications for Applied Analyses. In *Clustering and Classification*, pages 341–375. World Scientific Publishing Co, Singapore, 1996.

[70] Glenn W. Milligan and Martha C. Cooper. An examination of procedures for determining the number of clusters in a data set. *Psychometrika*, 50(2):159–179, 1985.

[71] Ashish Kumar Mishra and Biswarup Das. A Novel Density Based Clustering Approach for Electricity Theft Detection. *IEEE Transactions on Industry Applications*, PP:1–12, 2025.

[72] Botond Molnár, Ildikó Beáta Márton, Szabolcs Horvát, and Mária Ercsey Ravasz. Community detection in directed weighted networks using Voronoi partitioning. *Scientific Reports*, pages 1–19, 2024.

[73] Omid Motlagh, Adam Berry, and Lachlan O'Neil. Clustering of residential electricity customers using load time series. *Applied Energy*, 237(August 2018):11–24, 2019.

[74] Daniel Müllner. Fastcluster: Fast hierarchical, agglomerative clustering routines for R and Python. *Journal of Statistical Software*, 53(9):1–18, 2013.

[75] Tomoharu Nakashima, Gerald Schaefer, Youhei Kuroda, and Md. Atiqur Rahman Ahad. Performance evaluation of a two-stage clustering technique for time-series data. In *2016 5th International Conference on Informatics, Electronics and Vision (ICIEV)*, pages 1037–1040, 2016.

[76] Peggy M.L. Ng, Kam Kong Lit, and Cherry T.Y. Cheung. Remote work as a new normal? The technology-organization-environment (TOE) context. *Technology in Society*, 70(June):102022, 2022.

[77] Bryony Parrish, Phil Heptonstall, Rob Gross, and Benjamin K Sovacool. A systematic review of motivations , enablers and barriers for consumer engagement with residential demand response. *Energy Policy*, 138(January):111221, 2020.

[78] Ruobin Qi, Jun Zheng, Zhirui Luo, and Qingqing Li. A Novel Unsupervised Data-Driven Method for Electricity Theft Detection in AMI Using Observer Meters. *IEEE Transactions on Instrumentation and Measurement*, 71:1–10, 2022.

[79] Dawei Qiu, Yi Wang, Junkai Wang, Chuanwen Jiang, and Goran Strbac. Personalized retail pricing design for smart metering consumers in electricity market. *Applied Energy*, 348, 10 2023.

[80] Franklin L. Quilumba, Wei Jen Lee, Heng Huang, David Y. Wang, and Robert L. Szabados. Using smart meter data to improve the accuracy of intraday load forecasting considering customer behavior similarities. *IEEE Transactions on Smart Grid*, 6(2):911–918, 3 2015.

[81] Amin Rajabi, Mohsen Eskandari, Mojtaba Jabbari Ghadi, Li Li, Jiangfeng Zhang, and Pierluigi Siano. A comparative study of clustering techniques for electrical load pattern segmentation. *Renewable and Sustainable Energy Reviews*, 120:109628, 2020.

[82] Amin Rajabi, Li Li, Jiangfeng Zhang, Jianguo Zhu, Sahand Ghavidel, and Mojtaba Jabbari Ghadi. A review on clustering of residential electricity customers and its applications. *2017 20th International Conference on Electrical Machines and Systems, ICEMS 2017*, 2017.

[83] Thanawin Rakthanmanon, Bilson Campana, Abdullah Mueen, Gustavo Batista, Brandon Westover, Qiang Zhu, Jesin Zakaria, and Eamonn Keogh. Searching and mining trillions of time series subsequences under dynamic time warping. In *Proceedings of the ACM SIGKDD International Conference on Knowledge Discovery and Data Mining*, pages 262–270, Beijing, China, 2012. ACM.

[84] Elizabeth L. Ratnam, Steven R. Weller, Christopher M. Kellett, and Alan T. Murray. Residential load and rooftop PV generation: an Australian distribution network dataset. *International Journal of Sustainable Energy*, 36(8):787–806, 2017.

[85] Jörg Reichardt and Stefan Bornholdt. Statistical mechanics of community detection. *Phys. Rev. E*, 74(1):16110, 7 2006.

[86] Mohammad Rezaei and Pasi Franti. Set matching measures for external cluster validity. *IEEE Transactions on Knowledge and Data Engineering*, 28(8):2173–2186, 2016.

[87] Mike B Roberts, Navid Haghbadi, Anna Bruce, and Iain Macgill. Characterisation of Australian apartment electricity demand and its implications for low-carbon cities. *Energy*, 180(2019):242–257, 2020.

[88] Seunghyoun Ryu, Minsoo Kim, and Hongseok Kim. Denoising Autoencoder-Based Missing Value Imputation for Smart Meters. *IEEE Access*, 8:40656–40666, 2020.

[89] Hiroaki Sakoe and Seibi Chiba. Dynamic Programming Algorithm Optimization for Spoken Word Recognition. *IEEE Transactions on Acoustics, Speech, and Signal Processing*, 26(1):43–49, 1978.

[90] Claes Sandels, Marcus Kempe, Magnus Brolin, and Anders Mannikoff. Clustering Residential Customers with Smart Meter data using a Data Analytic Approach - External Validation and Robustness Analysis. *2019 9th International Conference on Power and Energy Systems, ICPES 2019*, 2019.

[91] Benjamin K. Sovacool, Andrew Hook, Siddharth Sareen, and Frank W. Geels. Global sustainability, innovation and governance dynamics of national smart electricity meter transitions. *Global Environmental Change*, 68:102272, 5 2021.

[92] Carlo Stagnaro. Second-generation smart meter roll-out in Italy: a cost–benefit analysis. *Journal of Industrial and Business Economics*, 52(1):201–220, 2024.

[93] D. B. Steffelbauer, E. J. M. Blokker, S. G. Buchberger, A. Knobbe, and E. Abraham. Dynamic Time Warping Clustering to Discover Socioeconomic Characteristics in Smart Water Meter Data. *Journal of Water Resources Planning and Management*, 147(6):1–12, 2021.

[94] Douglas Steinley. Properties of the Hubert-Arabie adjusted Rand index. *Psychological Methods*, 9(3):386–396, 9 2004.

[95] Li Sun, Kaile Zhou, and Shanlin Yang. An ensemble clustering based framework for household load profiling and driven factors identification. *Sustainable Cities and Society*, 53(November 2019):101958, 2020.

[96] Abdel Aziz Taha and Allan Hanbury. An Efficient Algorithm for Calculating the Exact Hausdorff Distance. *IEEE Transactions on Pattern Analysis and Machine Intelligence*, 37(11):2153–2163, 2015.

[97] Thanchanok Teeraratkul, Daniel O Neill, and Sanjay Lall. Shape-Based Approach to Household Electric Load Curve Clustering and Prediction. *IEEE Transactions on Smart Grid*, 9(5):5196–5206, 2018.

[98] Georg Thomaßen, Konstantinos Kavvadias, and Juan Pablo Jiménez Navarro. The decarbonisation of the EU heating sector through electrification: A parametric analysis. *Energy Policy*, 148(August 2020), 2021.

[99] Wiebke Toussaint and Deshendran Moodley. Comparison of clustering techniques for residential load profiles in South Africa. *CEUR Workshop Proceedings*, 2540:16, 2019.

[100] Wiebke Toussaint and Deshendran Moodley. Identifying optimal clustering structures for residential energy consumption patterns using competency questions. *ACM International Conference Proceeding Series*, 2020-Dec(December):66–73, 2020.

[101] V. A. Traag, P. Van Dooren, and Y. Nesterov. Narrow scope for resolution-limit-free community detection. *Physical Review E - Statistical, Nonlinear, and Soft Matter Physics*, 84(1):1–9, 2011.

[102] V. A. Traag, L. Waltman, and N. J. van Eck. From Louvain to Leiden: guaranteeing well-connected communities. *Scientific Reports*, 9(1):1–12, 2019.

[103] George J. Tsekouras, Nikos D. Hatzigyriou, and Evangelos N. Dialynas. Two-stage pattern recognition of load curves for classification of electricity customers. *IEEE Transactions on Power Systems*, 22(3):1120–1128, 8 2007.

[104] Alexander Tureczek, Per Sieverts Nielsen, and Henrik Madsen. Electricity consumption clustering using smart meter data. *Energies*, 11(4):1–18, 2018.

[105] Nguyen Xuan Vinh, Julien Epps, and James Bailey. Information theoretic measures for clusterings comparison: Variants, properties, normalization and correction for chance. *Journal of Machine Learning Research*, 11:2837–2854, 2010.

[106] Silke Wagner and Dorothea Wagner. Comparing Clusterings - An Overview. *Analysis*, 4769(001907):1–19, 2007.

[107] Hsin Chiao Wang and Yi Ling Chen. Long-Term Power Consumption Prediction with Two-Stage Clustering Framework. In *Proceedings of the International Joint Conference on Neural Networks*, volume 2023-June. Institute of Electrical and Electronics Engineers Inc., 2023.

[108] Liang Wang, Vignesh Narayanan, Yao Chi Yu, Yikyung Park, and Jr Shin Li. A Nested Two-Stage Clustering Method for Structured Temporal Sequence Data. *Knowledge and Information Systems*, 63(7):1627–1662, 7 2021.

[109] Xiaoyue Wang, Abdullah Mueen, Hui Ding, Goce Trajcevski, Peter Scheuermann, and Eamonn Keogh. Experimental comparison of representation methods and distance measures for time series data. *Data Mining and Knowledge Discovery*, 26(2):275–309, 2013.

[110] Yi Wang, Qixin Chen, Tao Hong, and Chongqing Kang. Review of Smart Meter Data Analytics : Applications , Methodologies , and Challenges. *IEEE Transactions on Smart Grid*, 10(3):3125–3148, 2019.

[111] Yi Wang, Qixin Chen, Chongqing Kang, and Qing Xia. Clustering of Electricity Consumption Behavior Dynamics Toward Big Data Applications. *IEEE Transactions on Smart Grid*, 7(5):2437–2447, 2016.

[112] Ebony Rose Watson, Ariane Mora, Atefeh Taherian Fard, and Jessica Cara Mar. How does the structure of data impact cell-cell similarity? Evaluating how structural properties influence the performance of proximity metrics in single cell RNA-seq data. *Briefings in Bioinformatics*, 23(6):1–14, 2022.

[113] Hanguan Wen, Xiufeng Liu, Ming Yang, Bo Lei, Xu Cheng, and Zhe Chen. An energy demand-side management and net metering decision framework. *Energy*, 271(February):127075, 2023.

[114] Xing Yan, Yusuf Ozturk, Zechun Hu, and Yonghua Song. A review on price-driven residential demand response. *Renewable and Sustainable Energy Reviews*, 96(April 2017):411–419, 2018.

[115] Luke W. Yerbury, Ricardo J. G. B. Campello, G. C. Livingston, Mark Goldsworthy, and Lachlan O’Neil. Comparing Clustering Approaches for Smart Meter Time Series: Investigating the Influence of Dataset Properties on Performance. *Applied Energy*, 391(August):125811, 2025.

[116] Luke W Yerbury, Ricardo J G B Campello, G C Livingston Jr., Mark Goldsworthy, and Lachlan O’Neil. On the Use of Relative Validity Indices for Comparing Clustering Approaches. *ACM Trans. Knowl. Discov. Data*, 19(8):53, 9 2025.

[117] S Yilmaz, J Chambers, and M K Patel. Comparison of clustering approaches for domestic electricity load profile characterisation - Implications for demand side management. *Energy*, 180:665–677, 2019.

[118] Meng Yuan, Jakob Zinck Thellufsen, Henrik Lund, and Yongtu Liang. The electrification of transportation in energy transition. *Energy*, 236, 2021.

[119] Liying Zhang, Tao Pei, Bin Meng, Yuanfeng Lian, and Zhou Jin. Two-phase multivariate time series clustering to classify urban rail transit stations. *IEEE Access*, 8:167998–168007, 2020.